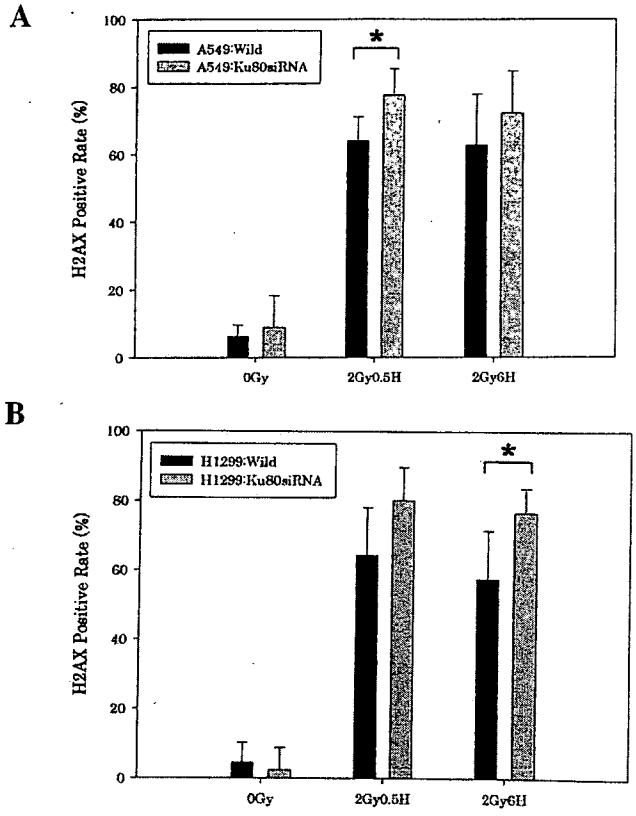

Figure 3. Positive rate of gamma-H2AX foci of A549 and H1299 cells stained 0.5 and 6 h after 2-Gy irradiation. In the A549 cells, the positive rate with siRNA treatment 0.5 h after irradiation is significantly higher than that with no siRNA treatment (p=0.033) (A). In the H1299 cells, the positive rate with siRNA treatment 6 h after irradiation is significantly higher than that with no siRNA treatment (p=0.026). Data are presented as the mean ± SE. H, hours (B).

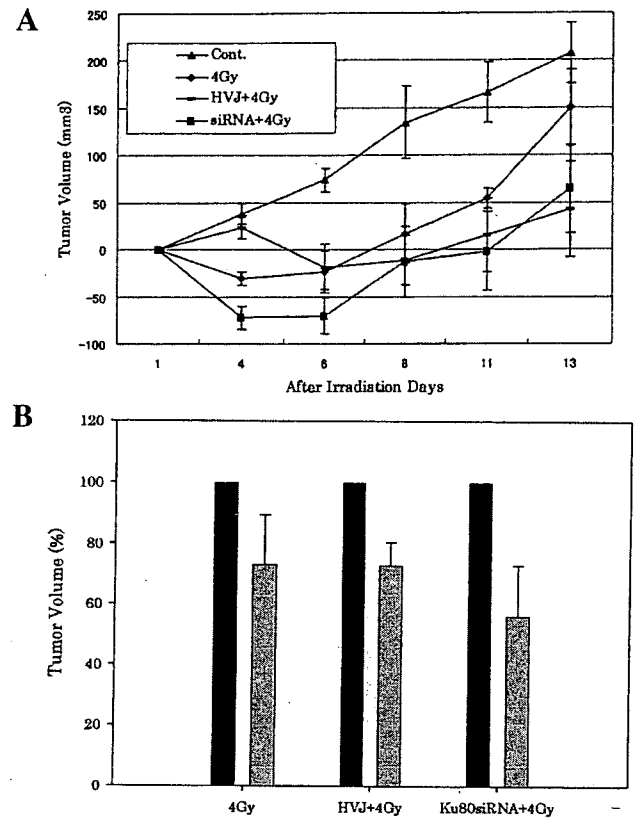

Figure 4. Enhanced tumor growth suppression by Ku80 siRNA combined with radiation therapy. Tumor growth curves for H1299 xenograft tumors treated with irradiation alone, HVJ-E vector, or Ku80 siRNA with irradiation. Quantification of H1299 xenograft increases (>0) or decreases (<0) tumor volumes compared with day 1 (A). The minimum volume of each tumor after irradiation was determined and calculated as a percentage in the various treatment groups compared with day 1 (100%) when the tumor was irradiated. Tumor volumes were measured two or three times weekly. Data are presented as the mean ± SE (B).

siRNA. When tumor volume reached 150-200 mm^3, the mice were randomly divided into four groups: control (n=5), radiation alone (n=4), HVJ-E vector treatment with radiation (n=5), and Ku80 siRNA treatment with radiation (n=6). After 4-Gy radiation, most tumors decreased in volume within 6 days and then began to increase again (Fig. 4A). Fig. 4B shows the percentage of the minimum volumes of each group compared with day 1 (100%). The rate of the reduction in volume of the tumors treated with Ku80 siRNA and radiation was the highest compared with the other groups. The scores of the remaining tumor were 72.95% for radiation alone, 72.70% for HVJ-E with radiation, and 56.02% for Ku80 siRNA with radiation. Even if one treatment was performed, an anti-tumor effect was expected from combination therapy with Ku80 siRNA and irradiation.

Delay in tumor growth by Ku80 siRNA for long-term observation. After confirming the suppression of tumor growth by Ku80 siRNA *in vivo*, the next goal was to follow for a long period the tumors treated with one fraction. When tumor volume reached 150-200 mm^3, the mice were randomly divided into three groups: control (n=11), radiation alone (n=6), and Ku80 siRNA treatment with radiation (n=6). The volume of the tumors in the two groups treated with radiation alone and combination therapy with Ku80 siRNA decreased until day 6 and re-grew in almost parallel fashion (Fig. 5A). By day 32, the increased volume of tumors treated with radiation alone was 404.4±60.2 mm^3 and that of combination therapy with Ku80 siRNA was 308.5±38.2 mm^3, indicating that tumor treated with combination therapy decreased to 76% of the volume of those treated with radiation alone.

The next trial consisted of 5 days of irradiation. To irradiate with five fractions, we waited until the tumor volume reached 750-1000 mm^3, at which point the mice were randomly divided into three groups: control (n=10), radiation alone (n=7), and Ku80 siRNA treatment with radiation (n=8). Irradiation was administered from days 1-5, and Ku80 siRNA was injected into the tumors on days 2 and 4. Until day 15, there was no difference in tumor growth in the two groups, which were treated with radiation alone and combined Ku80 siRNA. After day 15, combination therapy with Ku80 siRNA and radiation resulted in delayed tumor growth (Fig. 5B). By day 32, the increased tumor volume after treatment with five fractions alone was 1476.4±412.5 mm^3 and that of five fractions with two Ku80 siRNA treatments was 830.9±93.8 mm^3, indicating that Ku80 siRNA led to a 56% reduction in volume compared with radiation alone. For example, the proliferation time for the H1299 cell tumor to increase to ~900 mm^3 was

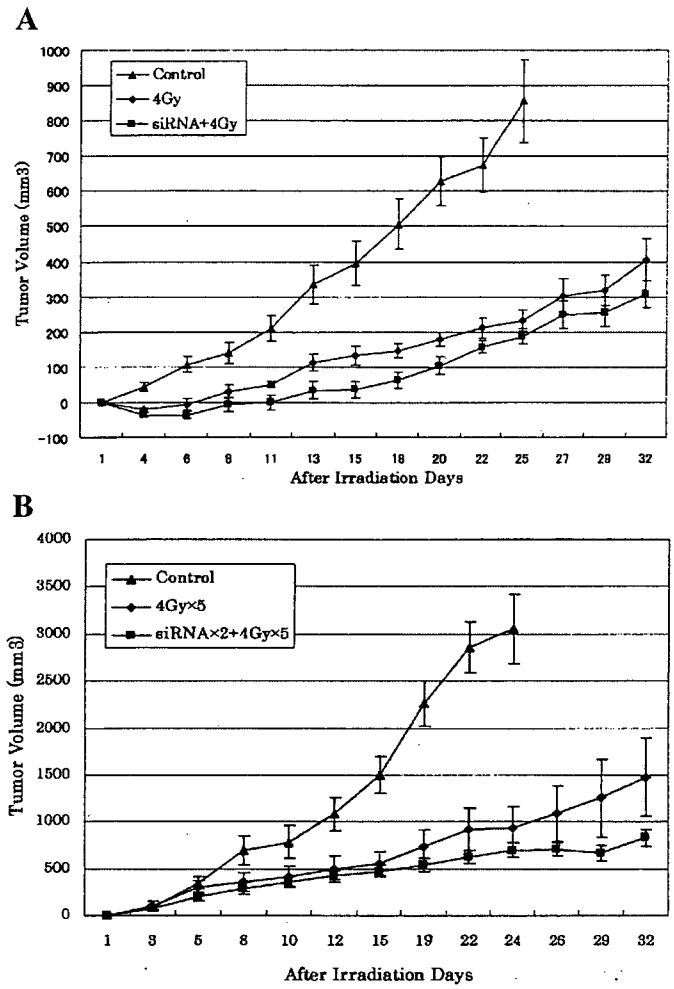

Figure 5. Growth delay curves of H1299 xenograft tumors treated with Ku80 siRNA and long-term irradiation. H1299 xenograft tumors were treated with one Ku80 siRNA treatment on day 0 and one fraction on day 1 (A). Tumors were treated with two Ku80 siRNA treatments on days 2 and 4 and five fractions from days 1 to 5. Data are presented as the mean ± SE (B).

about 22 days for the group treated with radiation alone. However, for the group treated with Ku80 siRNA and radiation, it took >32 days, which indicated a 10-day delay in tumor growth observed after using Ku80 siRNA.

Discussion

Ku80 plays an important role in repairing DNA DSBs, which are common in the DNA damage produced by irradiation (6). Ku was identified as an autoimmune antigen from the sera of a Japanese patient with scleroderma polymyosis overlap syndrome (28). An X-ray-sensitive mutant 5, xrs-5, was isolated from Chinese hamster ovary cell line (CHO K1) which was wild-type of Ku80 and extremely sensitive to irradiation (29). However, after transfection of Ku80 into xrs-5, the cells regained radiation resistance to the same level as CHO K1 (30). Therefore, we focused on Ku80 and hypothesized that silencing Ku80 might enhance radiation sensitivity and be advantageous in treating cancer with irradiation.

In this study, Ku80 protein was suppressed successfully by Ku80 siRNA *in vitro*. Although we chose Ku80 sequences, Ku70 protein expression also was suppressed after transfection with Ku80 siRNA. Loss of one Ku protein was reported to result in a significant decrease in the other Ku protein, because heterodimerization was required to stabilize each Ku protein (29). Furthermore, heterodimerization between Ku70 and Ku80 is essential for DSBs repair and also important in activation of DNA-PKs, which is a main function of Ku80 protein (3). Based on these facts, down-regulation of Ku80 protein by siRNA might have blocked heterodimerization with Ku70, thus inhibiting DNA repair after radiation.

We conducted an additional experiment to prove the inhibition of DNA DSBs repair after using Ku80 siRNA. Immunofluorescence detection of gamma-H2AX nuclear foci is used to detect DNA DSBs. The histone H2AX protein is a variant member of the H2A family of histones that is rapidly phosphorylated at the ser139 residue in response to radiation-induced DNA DSBs, resulting in the formation of nuclear foci (31-33). The prolonged and multiple expressions of H2AX foci after irradiation suggests decreased repair of DNA DSBs (32). Thus, immunofluorescence detection of gamma-H2AX nuclear foci was performed to visualize radiation-induced DSBs after treatment with Ku80 siRNA and to investigate why the radiation sensitivity increased. As expected, combination therapy resulted in enhanced radiation sensitivity. This effect correlated with gamma-H2AX staining, suggesting that the enhanced radiation sensitivity resulted from suppression of the Ku80 protein, which inhibited the ability of the DNA DSBs to repair themselves.

siRNA is expected to be the new therapeutic agent for cancer treatment (9-14). Although various procedures, for example, intravenous and direct injection, are being considered, the important issue is how the anti-tumor effect is acquired efficiently. In the current study, we selected the HVJ-E vector, which has been reported to be a new tool for the transfection reagents and was evaluated as useful and safe *in vitro* and *in vivo* (21-23). We also focused on injecting siRNA included in the HVJ-E vector directly into the tumor *in vivo*. The HVJ-E vector has been extremely safe to handle and efficient for gene transfer, and it might be a powerful candidate for future clinical use.

When cells were transfected with Ku80 siRNA by HVJ-E, Ku80 protein suppression was observed between 18 and 96 h after transfection (data not shown). Thus, we selected 40 h *in vitro* and 20 h *in vivo* after transfection for initiating treatment with radiation therapy to optimize the efficacy. When we used five fractions *in vivo*, we injected siRNA on days 2 and 4, which was 20 h before the radiation on days 3 and day 5. Ito *et al* reported that Rad51 siRNA suppressed protein expression in HeLa cells between 1 and 4 days after transfection and enhanced sensitivity to cisplatin during that period (17). Although each siRNA and cells have their own ability and characteristics, siRNA usually prevents protein expression for a few days; thus, the best timing must be considered for the combination therapy based on efficacy.

In the current study, the cells were treated with one transfection of Ku80 siRNA and one session of irradiation *in vitro*. Even if one treatment was administered, combination therapy with Ku80 siRNA and irradiation obviously enhanced

radiation sensitivity in several types of cancer cell lines. *In vivo*, H1299 xenograft tumors were treated twice with siRNA and five fractions, and the tumor volume decreased compared with radiation alone. However, most patients receive more than 20 fractions in normal clinical practice. So, in the future, we have to establish a regimen close to the clinical protocol, i.e., several treatments with Ku80 siRNA and irradiation.

Since not only malignant tumor cells but also normal tissues are exposed, there are many restrictions in the irradiation procedures, e.g., radiation times and tumor location. If the Ku80 expression in the tumor is inhibited by siRNA and the treatment that enhances radiation sensitivity can be performed for the patients, we may expect improvement in the efficiency of radiation therapy. Furthermore, the indication also may be extended to tumors that have not been targets of radiation therapy.

We showed that Ku80 siRNA included in the HVJ-E vector enhanced the radiation sensitivity of several human cancer cell lines regardless of the cancer type and radiation survival rate *in vitro*. Furthermore, radiation therapy combined with Ku80 siRNA resulted in inhibited tumor growth *in vivo*. Our results indicated that the combination of Ku80 siRNA and irradiation may be a useful novel strategy for cancer treatment considering the biological characteristics.

Acknowledgments

The authors are grateful to Drs Craig W. Stevens and Masaki Takiguchi for support. This study was financially supported by the 21st Century Center of Excellent program at Chiba University, and Grant-in-Aid for Scientific Research on Priority Areas (C) (grant numbers 16591189 and 17591250).

References

1. Haber JE: Partners and pathways repairing a double-strand break. Trends Genet 16: 259-264, 2000.
2. Hoeijmakers JH: Genome maintenance mechanisms for preventing cancer. Nature 411: 366-374, 2001.
3. Jin S and Weaver DT: Double-strand break repair by Ku70 requires heterodimerization with Ku80 and DNA binding functions. EMBO J 16: 6874-6885, 1997.
4. Nick McElhinny SA, Snowden CM, McCarville J and Ramsden DA: Ku recruits the XRCC4-ligase IV complex to DNA ends. Mol Cell Biol 20: 2996-3003, 2000.
5. Bassing CH, Swat W and Alt FW: The mechanism and regulation of chromosomal V(D)J recombination. Cell 109: S45-S55, 2002.
6. Ramsden DA and Gellert M: Ku protein stimulates DNA end joining by mammalian DNA ligases: a direct role for Ku in repair of DNA double-strand breaks. EMBO J 17: 609-614, 1998.
7. Nussenzweig A, Chen C, da Costa Soares V, Sanchez M, Sokol K, Nussenzweig MC and Li GC: Requirement for Ku80 in growth and immunoglobulin V(D)J recombination. Nature 382: 551-555, 1996.
8. Zhu C, Bogue MA, Lim DS, Hasty P and Roth DB: Ku86-deficient mice exhibit severe combined immunodeficiency and defective processing of V(D)J recombination intermediates. Cell 86: 379-389, 1996.
9. Zhang X, Chen ZG, Choe MS, Lin Y, Sun SY, Wieand HS, Shin HJ, Chen A, Khuri FR and Shin DM: Tumor growth inhibition by simultaneously blocking epidermal growth factor receptor and cyclooxygenase-2 in a xenograft model. Clin Cancer Res 11: 6261-6269, 2005.
10. Gao L, Zhang L, Hu J, Li F, Shao Y, Zhao D, Kalvakolanu DV, Kopecko DJ, Zhao X and Xu DQ: Down-regulation of signal transducer and activator of transcription 3 expression using vector-based small interfering RNAs suppresses growth of human prostate tumor *in vivo*. Clin Cancer Res 11: 6333-6341, 2005.
11. Ito T, Hashimoto Y, Tanaka E, Kan T, Tsunoda S, Sato F, Higashiyama M, Okumura T and Shimada Y: An inducible short-hairpin RNA vector against osteopontin reduces metastatic potential of human esophageal squamous cell carcinoma *in vitro* and *in vivo*. Clin Cancer Res 12: 1308-1316, 2006.
12. Halder J, Kamat AA, Landen CN Jr, Han LY, Lutgendorf SK, Lin YG, Merritt WM, Jennings NB, Chavez-Reyes A, Coleman RL, Gershenson DM, Schmandt R, Cole SW, Lopez-Berestein G and Sood AK: Focal adhesion kinase targeting using *in vivo* short interfering RNA delivery in neutral liposomes for ovarian carcinoma therapy. Clin Cancer Res 12: 4916-4924, 2006.
13. Amarzguioui M, Peng Q, Wiiger MT, Vasovic V, Babaie E, Holen T, Nesland JM and Prydz H: *Ex vivo* and *in vivo* delivery of anti-tissue factor short interfering RNA inhibits mouse pulmonary metastasis of B16 melanoma cells. Clin Cancer Res 12: 4055-4061, 2006.
14. Hosaka S, Nakatsura T, Tsukamoto H, Hatayama T, Baba H and Nishimura Y: Synthetic small interfering RNA targeting heat shock protein 105 induces apoptosis of various cancer cells both *in vitro* and *in vivo*. Cancer Sci 97: 623-632, 2006.
15. Peng Y, Zhang Q, Nagasawa H, Okayasu R, Liber HL and Bedford JS: Silencing expression of the catalytic subunit of DNA-dependent protein kinase by small interfering RNA sensitizes human cells for radiation-induced chromosome damage, cell killing, and mutation. Cancer Res 62: 6400-6404, 2002.
16. Collis SJ, Swartz MJ, Nelson WG and De Weese TL: Enhanced radiation and chemotherapy-mediated cell killing of human cancer cells by small inhibitory RNA silencing of DNA repair factors. Cancer Res 63: 1550-1554, 2003.
17. Ito M, Yamamoto S, Nimura K, Hiraoka K, Tamai K and Kaneda Y: Rad51 siRNA delivered by HVJ envelope vector enhances the anti-cancer effect of cisplatin. J Gene Med 7: 1044-1052, 2005.
18. Zhang Y, Lim CUK, Williams ES, Zhou J, Zhang Q, Fox MH, Bailey SM and Liber HL: *NBS1* knockdown by small interfering RNA increases ionizing radiation mutagenesis and telomere association in human cells. Cancer Res 65: 5544-5553, 2005.
19. Ohnishi K, Scuric Z, Schiestl RH, Okamoto N, Takahashi A and Ohnishi T: siRNA targeting *NBS1* or *XIAP* increases radiation sensitivity of human cancer cells independent of *TP53* satus. Radiat Res 166: 454-462, 2006.
20. Xu M, Myerson RJ, Hunt C, Kumar S, Moros EG, Straube WL and Roti JL: Transfection of human tumor cells with Mre11 siRNA and the increase in radiation sensitivity and the reduction in heat-induced radiosensitization. Int J Hyperthermia 20: 157-162, 2004.
21. Kaneda Y, Nakajima T, Nishikawa T, Yamamoto S, Ikegami H, Suzuki N, Nakamura H, Morishita R and Kotani H: Hemagglutinating virus of Japan (HVJ) envelope vector as a versatile gene delivery system. Mol Ther 6: 219-226, 2002.
22. Shimamura M, Morishita R, Endoh M, Oshima K, Aoki M, Waguri S, Uchiyama Y and Kaneda Y: HVJ-envelope vector for gene transfer into central nervous system. Biochem Biophys Res Commun 300: 464-471, 2003.
23. Nakamura H, Kimura T, Ikegami H, Ogita K, Koyama S, Shimoya K, Tsujie T, Koyama M, Kaneda Y and Murata Y: Highly efficient and minimally invasive *in vivo* gene transfer to the mouse uterus using haemagglutinating virus of Japan (HVJ) envelope vector. Mol Hum Reprod 9: 603-609, 2003.
24. Kojima C, Hashimoto A, Yabuta I, Hirose M, Hashimoto S, Kanaho Y, Sumimoto H, Ikegami T and Sabe H: Regulation of Bin1 SH3 domain binding by phosphoinositides. EMBO J 23: 4413-4422, 2004.
25. Ohnuma K, Yamochi T, Uchiyama M, Nishibashi K, Yoshikawa N, Shimizu N, Iwata S, Tanaka H, Dang NH and Morimoto C: CD26 up-regulates expression of CD86 on antigen-presenting cells by means of caveolin-1. Proc Natl Acad Sci USA 101: 14186-14191, 2004.
26. Sumi K, Yokozeki H, Wu MH, Satoh T, Kaneda Y, Takeda K, Akira S and Nishioka K: *In vivo* transfection of a cis element 'decoy' against signal transducers and activators of the transcription 6 (STAT6) binding site ameliorates the response of contact hypersensitivity. Gene Ther 11: 1763-1771, 2004.
27. Nimura Y, Ismail SM, Kurimas A, Chen DJ and Stevens CW: DNA-PK and ATM are required for radiation-enhanced integration. Radiat Res 157: 562-567, 2002.

28. Mimori T, Akizuki M, Yamagata H, Inada S, Yoshida S and Homma M: Characterization of a high molecular weight acidic nuclear protein recognized by autoantibodies in sera from patients with polymyositis-scleroderma overlap. J Clin Invest 68: 611-620, 1981.
29. Singleton BK, Priestley A, Steingrimsdottir H, Gell D, Blunt T, Jackson SP, Lehmann AR and Jeggo PA: Molecular and biochemical characterization of xrs mutants defective in Ku80. Mol Cell Biol 17: 1264-1273, 1997.
30. Stevens CW, Stamato TD, Mauldin SK, Getts RC, Zeng M and Cerniglia GJ: Radiation-induced recombination is dependent on Ku80. Radiat Res 151: 408-413, 1999.
31. Rogakou EP, Boon C, Redon C and Bonner WM: Megabase chromatin domains involved in DNA double strand breaks *in vivo*. J Cell Biol 146: 905-916, 1999.
32. Rothkamm K, Krüger I, Thompson LH and Lobrich M: Pathways of DNA double-strand break repair during the mammalian cell cycle. Mol Cell Biol 23: 5706-5715, 2003.
33. Camphausen K, Burgan W, Cerra M, Oswald KA, Trepel JB, Lee MJ and Tofilon PJ: Enhanced radiation-induced cell killing and prolongation of γ-H2AX foci expression by the histone deacetylase inhibitor MS-275. Cancer Res 64: 316-321, 2004.

Oncogene (2007) 26, 5669–5673

www.nature.com/onc

SHORT COMMUNICATION

DFF45/ICAD restores cisplatin-induced nuclear fragmentation but not DNA cleavage in *DFF45*-deficient neuroblastoma cells

M Takahashi[1,2], T Ozaki[1], A Takahashi[1,3], M Miyauchi[4], S Ono[3], N Takada[1,2], T Koda[3], S Todo[2], T Kamijo[1] and A Nakagawara[1]

[1]*Division of Biochemistry, Chiba Cancer Center Research Institute, Chuoh-ku, Chiba, Japan;* [2]*Department of General Surgery, Hokkaido University School of Medicine, Kita-ku, Sapporo, Japan;* [3]*Center for Functional Genomics, Hisamitsu Pharmaceutical Co., Inc., Chuoh-ku, Chiba, Japan and* [4]*Division of Pathology, Chiba Cancer Center Research Institute, Chuoh-ku, Chiba, Japan*

We have previously defined a homozygously deleted region at chromosome 1p36.2–p36.3 in human neuroblastoma cell lines, NB-1 and NB-C201, and identified six genes including *DFF45/ICAD* within this region. In this study, we found that NB-C201 cells are much more resistant to various genotoxic stresses such as cisplatin (CDDP) than CHP134 and SH-SY5Y cells that do not have the homozygous deletion. To examine a role(s) of DFF45 in the regulation of apoptosis in response to CDDP, we have established stably DFF45-expressing NB-C201 cell clones (DFF45-1 and DFF45-3) and a control cell clone (NB-C201-C) using a retrovirus-mediated gene transfer. In contrast to NB-C201-C cells, DFF45-3 cells displayed apoptotic nuclear fragmentation in response to CDDP. Although CDDP-induced proteolytic cleavage of procaspase-3 and DFF45 in DFF45-3 cells, we could not detect a typical apoptotic DNA fragmentation. Additionally, deletion analysis revealed that C-terminal region of DFF45 is required for inducing nuclear fragmentation. Unexpectedly, (3-(4,5-dimethylthiazol-2-yl)-2,5-diphenyltetrazolium bromide (MTT) assays demonstrated that DFF45 has undetectable effect on CDDP sensitivity of NB-C201 cells. Taken together, our present results suggest that DFF45/DFF40 system may be sufficient for CDDP-induced nuclear fragmentation but not DNA cleavage.

Oncogene (2007) **26,** 5669–5673; doi:10.1038/sj.onc.1210352; published online 12 March 2007

Keywords: apoptosis; cisplatin; DFF45/ICAD; homozygous deletion; neuroblastoma

Neuroblastoma (NBL) is one of the most common pediatric solid tumors and displays various clinical behaviors (Brodeur and Nakagawara, 1992). Loss at the distal part of the short arm of chromosome 1 (1p) and the amplification of *MYCN* in NBL are strongly associated with an unfavorable prognosis (Brodeur *et al.*, 1984). Extensive loss of heterozygosity (LOH) analysis narrowed the overlapping deleted region of 1p in NBL, suggesting that there could be at least three NBL suppressor loci (Schleiermacher *et al.*, 1994; Takeda *et al.*, 1994; Amler *et al.*, 1995; Cheng *et al.*, 1995; Martinsson *et al.*, 1995; White *et al.*, 1995). We found that NBL cell lines, NB-1 and NB-C201, carry a homozygous deletion at 1p36.2, and identified six genes within this region including *DFF45/ICAD*, *PGD*, *CORT*, *UFD2a*, *KIF1B-β* and *PEX14* (Ohira *et al.*, 2000). Among them, we have demonstrated that UFD2a promotes the proteasome-dependent degradation of p73 (Hosoda *et al.*, 2005).

Apoptosis is defined by a series of morphological and biochemical changes. DNA fragmentation is one of characteristic features of apoptosis (Raff, 1992) and triggered by a heterodimeric DNA fragmentation factor (DFF), which is composed of DFF40/CAD/CPAN nuclease and its inhibitor DFF45/ICAD. Upon apoptotic stimuli, DFF45 is cleaved by caspase-3 into three fragments and dissociates from DFF40, resulting in the activation of DFF40 (Liu *et al.*, 1997, 1998; Enari *et al.*, 1998; Halenbeck *et al.*, 1998; Mukae *et al.*, 1998; Sakahira *et al.*, 1998). DFF45 also acts as a folding chaperone required to produce active DFF40 (Enari *et al.*, 1998; Sakahira *et al.*, 1998). In this study, we examined a role(s) of DFF45 in the regulation of NBL cell death.

To assess the biological significance of the above-mentioned six genes, we compared the drug sensitivity of NBL cells with or without the homozygous deletion. NB-C201, CHP134 and SH-SY5Y cells were exposed to various genotoxic agents including cisplatin (CDDP), adriamycin (ADR) or etoposide (VP16), and their viability was monitored by (3-(4,5-dimethylthiazol-2-yl)-2,5-diphenyltetrazolium bromide (MTT) assay. As shown in Figure 1a, NB-C201 cells were much more resistant to CDDP, ADR and VP16 compared with CHP134 and SH-SY5Y cells. In accordance with these results, NB-C201 cells showed chromatin condensation in response to CDDP; however, nuclear fragmentation, which is one of morphological hallmarks of apoptosis (Wyllie, 1980), was undetectable in NB-C201 cells exposed to CDDP (Figure 1b). As DFF45-deficient cells showed a decreased

Correspondence: Dr A Nakagawara, Division of Biochemistry, Chiba Cancer Center Research Institute, 666-2 Nitona, Chuoh-ku, Chiba 260-8717, Japan.
E-mail: akiranak@chiba-cc.jp
Received 17 July 2006; revised 22 January 2007; accepted 23 January 2007; published online 12 March 2007

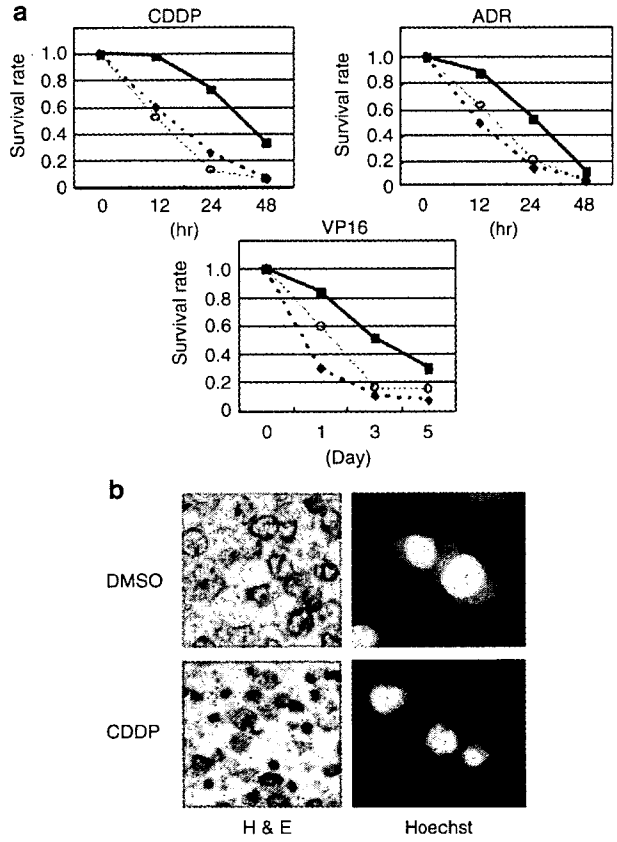

Figure 1 CDDP sensitivity of *DFF45*-deficient NBL cell. (**a**) Effect of various genotoxic agents on NBL cells. NB-C201 (■), CHP134 (◆) and SH-SY5Y (□) cells were treated with CDDP (25 μM), ADR (1 μg/ml) or VP16 (50 μM). At the indicated time periods, cell viability was determined by MTT assays. Data are shown as the number of viable cells relative to that of untreated cells, which is arbitrarily assigned a value of 1.0. (**b**) Chromatin condensation of CDDP-treated NB-C201 cells. NB-C201 cells were exposed to DMSO (top panels) or 25 μM of CDDP (bottom panels) for 24 h. Cells were processed for hematoxylin and eosin (H&E) staining (left panels) or stained with Hoechst dye to reveal the degree of chromatin condensation (right panels).

sensitivity to apoptotic stimuli (Zhang *et al*., 1999), we tested a possibility that the lack of DFF45 is responsible for the drug resistance of NBL cells. We first examined the expression of *DFF45* and *DFF40* in various NBL cell lines by Northern blot analysis. HeLa cells were used as a positive control (Liu *et al*., 1997). As reported (Ohira *et al*., 2000), *DFF45* was undetectable in NB-1 and NB-C201 cells, whereas variable levels of *DFF45* were detected in the remaining cells (Figure 2a, top panel). Previous results indicated that *DFF45* is expressed as two transcripts of 3.8 and 2.4 kb in length (Zhang *et al*., 1999). However, Yang *et al*. (2001) described that some different-sized mRNAs are expressed in several NBL cell lines. We observed four *DFF45* transcripts of 5.4, 3.8, 2.4 and 1.6 kb in length. On the other hand, a single *DFF40* transcript (3.4 kb) was detectable in all NBL cell lines (Figure 2a, middle panel) as reported in other cell types (Mukae *et al*., 1998). Immunoblot analysis also revealed that substantial amounts of DFF45 and DFF40 are expressed in SH-SY5Y and CHP134 cells, whereas NB-C201 cells express DFF40 but not DFF45 (Figure 2b).

To explore the role of DFF45 in response to CDDP, the retroviral vector encoding DFF45 was introduced into NB-C201 cells and stable cell clones were established. As shown in Figure 2c, DFF45-1, -3, -4, -7, and -8 clones expressed relatively larger amounts of DFF45 compared with the remaining clones. DFF45 was not detectable in NB-C201 cells infected with an empty vector (NB-C201-C). The enforced expression of DFF45 did not affect the expression levels of DFF40 (Figure 2d). We employed DFF45-1 and DFF45-3 cells for further experiments. Consistent with the previous observations (Liu *et al*., 1998), exogenously expressed DFF45 was largely localized in cell nucleus (Figure 2e). We then examined whether DFF45 could affect CDDP sensitivity of NB-C201 cells. NB-C201-C, DFF45-1 and DFF45-3 cells were treated with CDDP for the indicated time periods and their viability was measured by the MTT assay. Unexpectedly, DFF45 had no detectable effects on the viability of NB-C201 cells in response to CDDP (Figure 2f).

We then addressed whether DFF45 could affect the nuclear morphology in response to CDDP. NB-C201-C and DFF45-3 cells were exposed to CDDP for 48 h and their nuclear morphology was examined. As seen in Figure 3a, Hoechst staining clearly demonstrated that apoptotic nuclear fragmentation takes place in DFF45-3 cells, but not in NB-C201-C cells. These results were confirmed by electron microscopic analysis (Figure 3b). Similar results were also obtained in DFF45-1 cells (data not shown). We sought to examine whether DFF45 could promote DNA fragmentation in response to CDDP by TUNEL staining. CDDP-sensitive CHP134 cells were used as a positive control. Unexpectedly, we observed no TUNEL-positive nuclei in DFF45-3 cells (Figure 3c). DNA fragmentation as assessed by agarose gel electrophoresis did not occur in DFF45-3 cells exposed to CDDP. As described previously (Enari *et al*., 1998; Liu *et al*., 1998), caspase-3-dependent cleavage of DFF45 was required for the activity of DFF40. We therefore addressed a possibility that caspase-3-mediated cleavage of DFF45 could be impaired owing to a loss of the activation of caspase-3 in DFF45-3 cells in response to CDDP. As shown in Figure 3e, the time-dependent cleavage of procaspase-3 and DFF45 was observed in DFF45-3 cells. Thus, DFF45 induced nuclear fragmentation, but not DNA fragmentation in NB-C201 cells.

We then examined whether the region(s) of DFF45 involved in nuclear fragmentation could be distinct from that required for DNase activity. To this end, we constructed a series of FLAG-tagged DFF45 deletion mutants (Figure 4a) and then introduced them into NB-C201 cells. After 2 weeks of culture in the presence of G418, drug-resistant colonies were combined and expanded. As shown in Figure 4b, each vector gave rise to a stable protein with the expected size. CDDP-induced nuclear fragmentation in NB-C201 cells expressing wild-type DFF45, whereas DFF45 (1–290), DFF45 (1–231) or

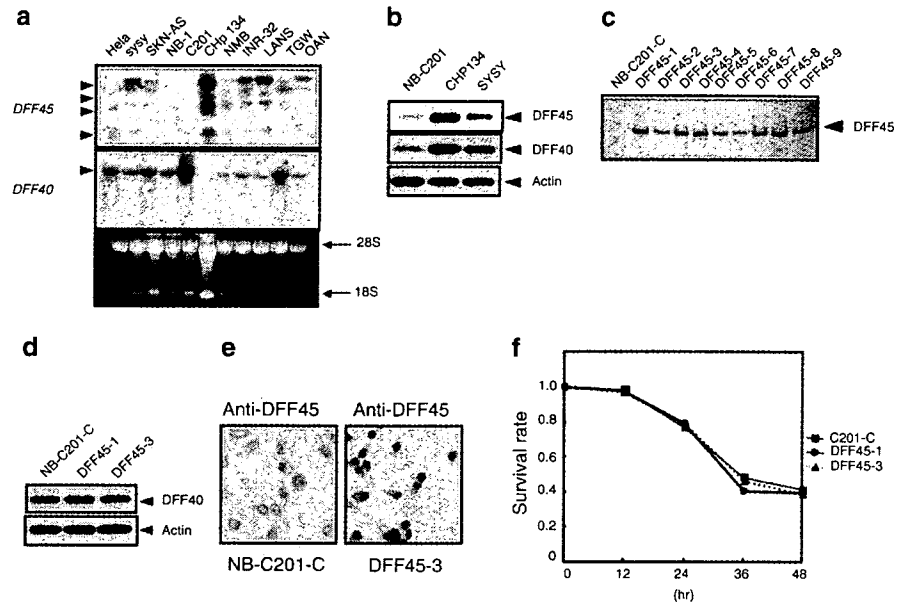

Figure 2 Enforced expression of DFF45 in NB-C201 cells. (**a**) Expression of *DFF45* and *DFF40* in various NBL cell lines. Total RNA from the indicated cells was subjected to Northern blot analysis using the radiolabeled *DFF45* (top panel) or *DFF40* (middle panel) cDNA. Relative RNA loading is indicated by the intensity of the 18S and 28S rRNA bands (bottom panel). (**b**) Expression of DFF45 and DFF40 in NBL cells. Lysates from the indicated cells were processed for immunoblotting with anti-DFF45 (top panel) or anti-DFF40 (middle panel) antibody. (**c**) Immunoblot analysis. Lysates from the indicated cell clones were subjected to immunoblotting with anti-DFF45 antibody. (**d**) Expression of DFF40 in stable cell clones. Lysates from the indicated cell clones were subjected to immunoblotting with anti-DFF40 antibody. (**e**) Immunostaining. Four-micrometer sections of paraffin-embedded, formaldehyde-fixed NB-C201-C (left panel) and DFF45-3 (right panel) cells were deparaffinized in xylene, rehydrated through a series of ethanol and then stained with anti-DFF45 antibody. (**f**) Effects of DFF45 on CDDP sensitivity. NB-C201-C (■), DFF45-1 (•) and DFF45-3 (▲) cells were treated with 25 μM of CDDP. At the indicated time periods, cell viability was measured by MTT assays.

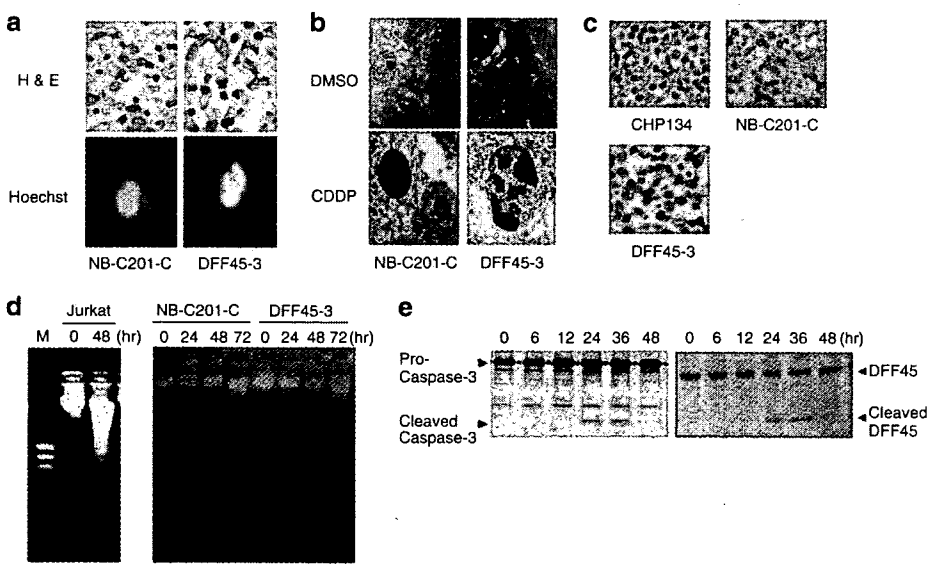

Figure 3 DFF45 promotes nuclear fragmentation but not DNA fragmentation. (**a**) Nuclear fragmentation of CDDP-treated DFF45-3 cells. NB-C201-C (left panels) and DFF45-3 (right panels) cells were exposed to 25 μM of CDDP. Forty-eight hours after treatment, cells were stained with H&E (top panels) or with Hoechst dye (bottom panels). (**b**) Electron micrographs. NB-C201-C (left panels) and DFF45-3 (right panels) cells were exposed to 25 μM of CDDP (bottom panels) or left untreated (top panels). Forty-eight hours after CDDP treatment, NB-C201-C and DFF45-3 cells were fixed, embedded with an epoxy resin, and grid-mounted sections were then processed for transmission electron microscopy. (**c**) TUNEL staining. CHP134, NB-C201-C and DFF45-3 cells were treated with 25 μM of CDDP. Forty-eight hours after CDDP treatment, cells were stained for TUNEL (Roche Applied Science, Indianapolis, IN, USA). (**d**) DNA fragmentation assay. Jurkat, NB-C201-C and DFF45-3 cells treated with CDDP (25 μM) for the indicated time periods were used for genomic DNA preparation. After RNase A treatment, genomic DNA was subjected to 1.5% agarose gel electrophoresis and visualized under ultraviolet light. (**e**) Caspase-3 activation in response to CDDP. DFF45-3 cells were exposed to 25 μM of CDDP. At the indicated time points after the drug exposure, lysates were subjected to immunoblotting with anti-caspase-3 (Pharmingen, San Jose, CA, USA) (left panel) or anti-DFF45 (C-19; Santa Cruz Biotechnology, Santa Cruz, CA, USA) (right panel) antibody.

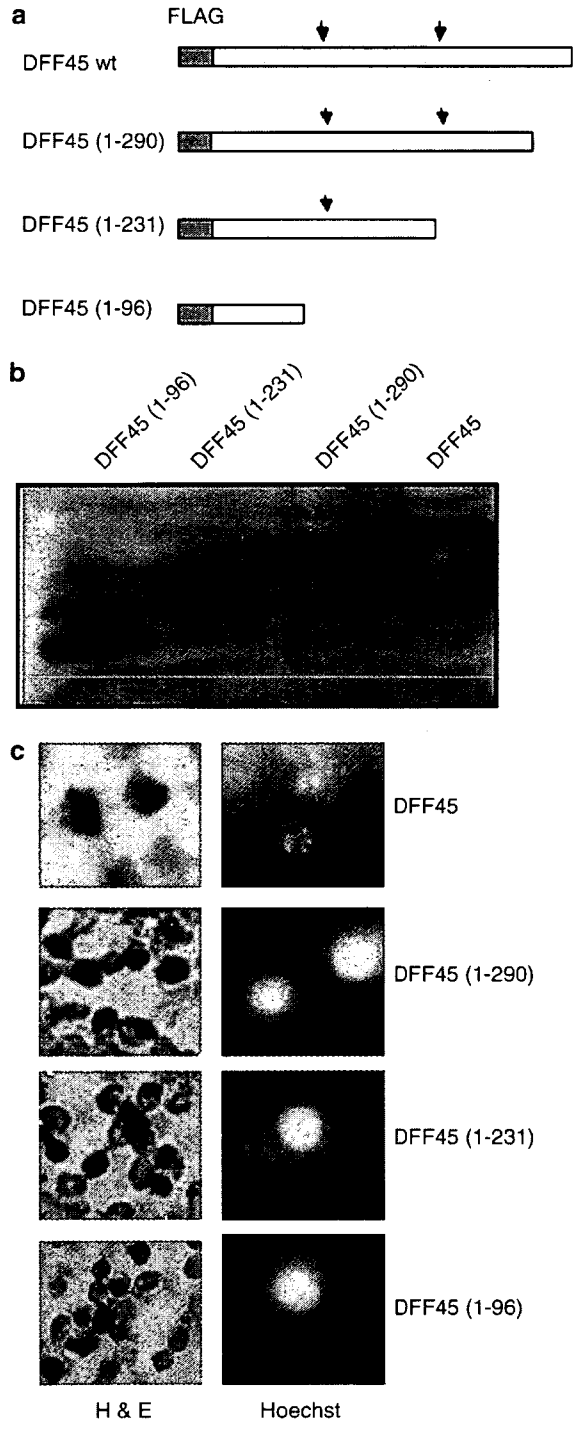

Figure 4 C-terminal region of DFF45 is required for CDDP-induced nuclear fragmentation. (**a**) Schematic representation of a series of FLAG-tagged deletion mutants of DFF45. Closed arrowheads indicate the positions of caspase-3 cleavage sites. (**b**) Expression of DFF45 deletion mutants. Lysates from NB-C201 cells infected with the indicated retroviral vector were subjected to immunoblotting with anti-FLAG (M2; Sigma, St Louis, MO, USA) antibody. (**c**) Effect of DFF45 deletion mutants on nuclear morphology in the presence of CDDP. NB-C201 cells infected with the indicated retroviral vector were exposed to CDDP (25 μM) for 48 h. Cells were then stained with H&E (left panels) or with Hoechst dye to reveal the degree of nuclear fragmentation (right panels).

DFF45 (1–96) failed to induce nuclear fragmentation in response to CDDP (Figure 4c), suggesting that COOH-terminal region of DFF45 is essential for the induction of nuclear fragmentation in NB-C201 cells. As described by Gu *et al.* (1999), central domain of DFF45 (amino-acid residues 101–180) is required for the interaction with DFF40 and DFF45 can assist in the synthesis of highly active DFF40. In addition, the catalytic domain of DFF40 is located in its COOH-terminal region (amino-acid residues 290–345) (Inohara *et al.*, 1999). As our mutation searches revealed that NB-C201 cells express wild-type *DFF40* (data not shown), it is likely that CDDP-mediated nuclear fragmentation might be regulated in a DFF45- but not in a DFF40-dependent manner.

As described by Ohira *et al.* (2000), we failed to detect any mutations within *DFF45* in NBLs. Similar results were reported by Yang *et al.* (2001). In this study, we found that DFF45 can selectively restore the ability to induce nuclear fragmentation but not DNA cleavage in response to CDDP. Recently, it has been shown that γH2AX regulates DNA fragmentation mediated by DFF40 (Lu *et al.*, 2006). Our preliminary experiments revealed that the amounts of γH2AX remain unchanged regardless of CDDP treatment (data not shown). Moreover, chromatin condensation and nuclear fragmentation have been shown to be regulated by nucleoplasmin, indicating that nuclear morphological changes and DNA fragmentation are independent processes (Lu *et al.*, 2005). Further efforts should be devoted to delineate whether such dissociation of nucleolytic and DNase activities of DFF45/DFF40 system in a subset of NBL cells contributes to the highly variable clinical behavior of this neoplasm.

Acknowledgements

This work was supported in part by a Grant-in-Aid from the Ministry of Health, Labour and Welfare for Third Term Comprehensive Control Research for Cancer, and a Grant-in-Aid for Cancer Research from the Ministry of Health, Labour and Welfare of Japan, a Grant-in-Aid for Scientific Research on Priority Areas from the Ministry of Education, Culture, Sports, Science and Technology, Japan, and a grant from Uehara Memorial Foundation.

References

Amler LC, Corvi R, Praml C, Savelyeva L, Le Paslier D, Schwab M. (1995). A reciprocal translocation (1;15)(36.2;q24) in a neuroblastoma cell line is accompanied by DNA duplication and may signal the site of a putative tumor suppressor gene. *Oncogene* **10**: 1095–1101.

Brodeur GM, Seeger RC, Schwab M, Varmas HE, Bishop JM. (1984). Amplification of N-*myc* in untreated human neuroblastomas corelates with advanced disease stage. *Science* **224**: 1121–1124.

Brodeur GM, Nakagawara A. (1992). Molecular basis of clinical heterogeneity in neuroblastoma. *Am J Pediatr Hematol Oncol* **14**: 111–116.

Cheng NC, Van Roy N, Chan A, Beitsma M, Westerveld A, Speleman F *et al.* (1995). Deletion mapping in neuroblastoma cell lines suggests two distinct tumor suppressor genes

in the 1p35–36 region, only one of which is associated with N-myc amplification. *Oncogene* **10**: 291–297.

Enari M, Sakahira H, Yokoyama H, Okawa K, Iwamatsu A, Nagata S. (1998). A caspase-activated DNase that degrades DNA during apoptosis, and its inhibitor ICAD. *Nature* **391**: 43–50.

Gu J, Dong RP, Zhang C, McLaughlin DF, Wu MX, Schlossman SF. (1999). Functional interaction of DFF35 and DFF45 with caspase-activated DNA fragmentation nuclease DFF40. *J Biol Chem* **274**: 20759–20762.

Halenbeck R, MacDonald H, Roulston A, Chen TT, Conroy L, Williams LT. (1998). CPAN, a human nuclease regulated by the caspase-sensitive inhibitor DFF45. *Curr Biol* **8**: 537–540.

Hosoda M, Ozaki T, Miyazaki K, Hayashi S, Furuya S, Watanabe K *et al.* (2005). UFD2a mediates the proteasomal turnover of p73 without promoting p73 ubiquitination. *Oncogene* **24**: 7156–7169.

Inohara N, Koseki T, Chen S, Benedict MA, Nunez G. (1999). Identification of regulatory and catalytic domains in the apoptosis nuclease DFF40/CAD. *J Biol Chem* **274**: 270–274.

Liu X, Zou H, Slaughter C, Wang X. (1997). DFF, a heterodimeric protein that functions downstream of caspase-3 to trigger DNA fragmentation during apoptosis. *Cell* **89**: 175–184.

Liu X, Li P, Widlak P, Zou H, Luo X, Garrard WT *et al.* (1998). The 40-kDa subunit of DNA fragmentation factor induces DNA fragmentation and chromatin condensation during apoptosis. *Proc Natl Acad Sci USA* **95**: 8461–8466.

Lu C, Zhu F, Cho YY, Tang F, Zykova T, Ma WY *et al.* (2006). Cell apoptosis: requirement of H2AX in DNA ladder formation, but not for the activation of caspase-3. *Mol Cell* **23**: 121–132.

Lu Z, Zhang C, Zhai Z. (2005). Nucleoplasmin regulates chromatin condensation during apoptosis. *Proc Natl Acad Sci USA* **102**: 2778–2783.

Martinsson T, Sjoberg RM, Hedborg F, Kogner P. (1995). Deletion of chromosome 1p loci and microsatellite instability in neuroblastomas analyzed with short-tandem repeat polymorphisms. *Cancer Res* **55**: 5681–5686.

Mukae N, Enari M, Sakahira H, Fukuda Y, Inazawa J, Tho H *et al.* (1998). Molecular cloning and characterization of human caspase- activated DNase. *Proc Natl Acad Sci USA* **95**: 9123–9128.

Ohira M, Kageyama H, Mihara M, Furuta S, Machida T, Shishikura T *et al.* (2000). Identification and characterization of a 500-kb homozygously deleted region at 1p36.2–p36.3 in a neuroblastoma cell line. *Oncogene* **19**: 4302–4307.

Raff MC. (1992). Social controls on cell survival and cell death. *Nature* **356**: 397–400.

Sakahira H, Enari M, Nagata S. (1998). Cleavage of CAD inhibitor in CAD activation and DNA degradation during apoptosis. *Nature* **391**: 96–99.

Schleiermacher G, Peter M, Michon J, Hugot JP, Vielh P, Zucker JM *et al.* (1994). Two distinct deleted regions on the short arm of chromosome 1 in neuroblastoma. *Genes Chromosomes Cancer* **10**: 275–281.

Takeda O, Homma C, Maseki N, Sakurai M, Kanda N, Schwab M *et al.* (1994). There may be two tumor suppressor genes on chromosome arm 1p closely associated with biologically distinct subtypes of neuroblastoma. *Genes Chromosomes Cancer* **10**: 30–39.

White PS, Maris JM, Beltinger C, Sulman E, Marshall HN, Fujimori M *et al.* (1995). A region of consistent deletion in neuroblastoma maps within human chromosome 1p36.2–36.3. *Proc Natl Acad Sci USA* **92**: 5520–5524.

Wyllie AH. (1980). Glucocorticoid-induced thymocyte apoptosis is associated with endogenous endonuclease activation. *Nature* **284**: 555–556.

Yang HW, Chen YZ, Piao HY, Takita J, Soeda E, Hayashi Y. (2001). DNA fragmentation factor 45 (DFF45) gene at 1p36.2 is homozygously deleted and encodes variant transcripts in neuroblastoma cell line. *Neoplasia* **3**: 165–169.

Zhang J, Wang X, Bove KE, Xu M. (1999). DNA fragmentation factor 45-deficient cells are more resistant to apoptosis and exhibit different dying morphology than wild-type control cells. *J Biol Chem* **274**: 37450–37454.

THE JOURNAL OF BIOLOGICAL CHEMISTRY VOL. 282, NO. 25, pp. 18365–18378, June 22, 2007

Stabilization of p73 by Nuclear IκB Kinase-α Mediates Cisplatin-induced Apoptosis*

Received for publication, November 13, 2006, and in revised form, April 23, 2007 Published, JBC Papers in Press, April 23, 2007, DOI 10.1074/jbc.M610522200

Kazushige Furuya[‡§], Toshinori Ozaki[‡], Takayuki Hanamoto[‡], Mitsuchika Hosoda[‡], Syunji Hayashi[‡], Philip A. Barker[¶], Kunio Takano[§], Masahiko Matsumoto[§], and Akira Nakagawara[‡1]

From the [‡]Division of Biochemistry, Chiba Cancer Center Research Institute, Chiba 260-8717, Japan, the [§]Second Department of Surgery, Yamanashi University School of Medicine, Yamanashi 409-3898, Japan, and the [¶]Montreal Neurological Institute, McGill University, Montreal, Quebec H3A 2B4, Canada

In response to DNA damage, p53 and its homolog p73 have a function antagonistic to NF-κB in deciding cell fate. Here, we show for the first time that p73, but not p53, is stabilized by physical interaction with nuclear IκB kinase (IKK)-α to enhance cisplatin (CDDP)-induced apoptosis. CDDP caused a significant increase in the amounts of nuclear IKK-α and p73α in human osteosarcoma-derived U2OS cells. Ectopic expression of IKK-α prolonged the half-life of p73 by inhibiting its ubiquitination and thereby enhancing its transactivation and pro-apoptotic activities. Consistent with these results, small interfering RNA-mediated knockdown of endogenous IKK-α inhibited the CDDP-mediated accumulation of p73α. The kinase-deficient mutant form of IKK-α interacted with p73α, but failed to stabilize it. Furthermore, CDDP-mediated accumulation of endogenous p73α was not detected in mouse embryonic fibroblasts (MEFs) prepared from IKK-α-deficient mice, and CDDP sensitivity was significantly decreased in IKK-α-deficient MEFs compared with wild-type MEFs. Thus, our results strongly suggest that the nuclear IKK-α-mediated accumulation of p73α is one of the novel molecular mechanisms to induce apoptotic cell death in response to CDDP, which may be particularly important in killing tumor cells with *p53* mutation.

The NF-κB signaling pathway is activated by a variety of structurally and functionally unrelated stimuli, including inflammatory cytokines, ionizing radiation, viral and bacterial infection, and oxidative stress (reviewed in Refs. 1 and 2). Under normal conditions, NF-κB exists as heterodimeric complexes composed of p50 and p65 (RelA) subunits and is kept transcriptionally inactive through interaction with its inhibitory proteins such as IκB-α and IκB-β. IκB proteins mask the nuclear localization signal of NF-κB, thereby preventing its nuclear translocation. Upon certain stimulations, IκB proteins are rapidly phosphorylated at specific serine residues in the N-terminal their signal-responsive domain by upstream regulator IκB kinase (IKK)[2] complex and subsequently polyubiquitinated and degraded in a proteasome-dependent manner (reviewed in Ref. 3). The high molecular mass IKK complex comprises two related catalytic subunits, IKK-α (also called IKK-1) and IKK-β (also called IKK-2), and one regulatory subunit with a scaffold function, IKK-γ (also called NEMO) (reviewed in Ref. 3). The proteolytic degradation of IκB proteins exposes the nuclear localization signal of NF-κB and results in translocation of NF-κB from the cytoplasm to the nucleus, allowing it to participate in transcriptional regulation of numerous target genes involved in immune responses, inflammatory reactions, cell adhesion, cell proliferation, apoptotic cell death, and other cellular processes. Therefore, the IKK complex represents one of the critical upstream regulators of the NF-κB signaling pathway.

In many experimental systems, the activation of NF-κB has been shown to play an important role in the control of survival processes, protecting cells from a variety of apoptotic signals (4–8). For example, tumor necrosis factor-α (TNF-α) simultaneously activates the NF-κB-mediated cellular protective mechanism against the pro-apoptotic effect of TNF-α through the induction of the NF-κB-responsive genes that function to block apoptosis. Additionally, inhibition of NF-κB has been shown to enhance sensitivity to chemotherapeutic agents (9, 10). Consistent with the well documented anti-apoptotic effect of NF-κB, high levels of NF-κB activity are detectable in various human tumors (11). On the other hand, NF-κB activation results in the promotion of apoptosis, depending on different stimuli and cell types. Huang and Fan (12) reported that the activation of NF-κB contributes to paclitaxel-induced apoptosis in human solid tumor cells. In addition, Bian *et al.* (13) found that NF-κB activation mediates doxorubicin-induced apoptosis in N-type neuroblastoma cells. In both cases, treatment of cells with the cytotoxic agents significantly down-regulated cytoplasmic IκB-α and then promoted the nuclear transloca-

* This work was supported in part by a grant-in-aid for third term comprehensive control research for cancer from the Ministry of Health, Labor and Welfare, by a grant-in-aid for scientific research on priority areas from the Ministry of Education, Culture, Sports, Science and Technology of Japan, and by a grant-in-aid for scientific research from the Japan Society for the Promotion of Science. The costs of publication of this article were defrayed in part by the payment of page charges. This article must therefore be hereby marked "*advertisement*" in accordance with 18 U.S.C. Section 1734 solely to indicate this fact.

[1] To whom correspondence should be addressed: Div. of Biochemistry, Chiba Cancer Center Research Inst., 666-2 Nitona, Chuoh-ku, Chiba 260-8717, Japan. Tel.: 81-43-264-5431; Fax: 81-43-265-4459; E-mail: akiranak@chiba-cc.jp.

[2] The abbreviations used are: IKK, IκB kinase; TNF-α, tumor necrosis factor-α; CDDP, cisplatin; siRNA, small interfering RNA; MEFs, mouse embryonic fibroblasts; MTT, 3-(4,5-dimethylthiazol-2-yl)-2,5-diphenyltetrazolium bromide; RT, reverse transcription; GST, glutathione S-transferase; HA, hemagglutinin; PIPES, 1,4-piperazinediethanesulfonic acid; MOPS, 4-morpholinepropanesulfonic acid; CBP, cAMP-responsive element-binding protein-binding protein.

tion of NF-κB; however, the molecular mechanism of the pro-apoptotic effect of NF-κB is still largely unknown.

p73 belongs to a small family of p53-related nuclear transcription factors. In accordance with their structural similarity, p73 functions in a manner analogous to p53 by inducing G_1 cell cycle arrest or apoptosis in certain cancerous cells through transactivating an overlapping set of p53/p73 target genes (reviewed in Ref. 14). Like p53, endogenous p73 becomes stabilized as well as activated in cells exposed to certain genotoxic stimuli, including γ-irradiation and cisplatin (CDDP), and contributes to an apoptotic response to DNA damage (15–17). p73 is expressed as multiple isoforms that differ at their N and C termini, arising from alternative splicing and promoter usage (reviewed in Ref. 14). Among them, an N-terminally truncated form of p73 (ΔNp73) that lacks the transactivation domain of p73 has an oncogenic potential and exhibits dominant-negative behavior toward wild-type p73 as well as p53 (18–20). Of particular note, we (22) and others (21, 23) demonstrated that p73 directly transactivates the expression of its own negative regulator, ΔNp73, suggesting that a negative feedback regulation of p73 by ΔNp73 exists to modulate cell survival and death.

In response to primary antigenic stimulation, NF-κB limits the up-regulation of pro-apoptotic p73 in T cells, resulting in the promotion of T cell survival; however, the precise molecular basis by which NF-κB activation inhibits the expression of p73 remains to be determined (24). It is worth noting that IKK-β, but not IKK-α, activates NF-κB, thereby inhibiting the accumulation of p53 at the protein level in response to the anticancer agent doxorubicin (25). IκB-α might play a role in sequestering p53 in the cytoplasm through the physical interaction with p53, thereby preventing the nuclear translocation of p53 (26). These observations suggest that NF-κB activation might abrogate p53- and/or p73-mediated apoptosis. In marked contrast, Ryan *et al.* (27) reported that NF-κB is required for p53-dependent apoptosis. Additionally, it has been demonstrated that p53 is a direct transcriptional target of NF-κB and that the p53-activating signal is partially blocked by inhibition of NF-κB activation (28–30). In support of this notion, Fujioka *et al.* (31) reported that NF-κB acts as a pro-apoptotic factor by activating the p53 signaling pathway. However, the functional significance of the possible interplay between the NF-κB signaling pathway and p53- and/or p73-mediated apoptosis has not been established.

In addition to the role of the cytoplasmic IKK complex in regulating the signal-dependent induction of NF-κB target genes, Birbach *et al.* (32) found that one of its components (IKK-α) shuttles between the cytoplasm and nucleus of unstimulated cells, suggesting that IKK-α might have a novel nuclear role in controlling cell survival and death. Consistent with this notion, it has been shown that IKK-α accumulates in the cell nucleus in response to cytokine exposure and stimulates the expression of NF-κB-responsive genes through promoter-associated histone H3 phosphorylation (33, 34). In this study, we found that IKK-α accumulates in the cell nucleus during the CDDP-mediated apoptotic process. Moreover, IKK-α increased the stability of p73, but not p53, through direct interaction with p73 and enhanced p73-dependent transcriptional activity as well as pro-apoptotic function. Reduction of endogenous IKK-α by small interfering RNA (siRNA) against IKK-α resulted in the significant attenuation of the CDDP-induced accumulation of p73α. Similar results were also obtained in mouse embryonic fibroblasts (MEFs) derived from IKK-α-deficient mice (IKK-$\alpha^{-/-}$ MEFs). Thus, our findings suggest that IKK-α has a novel nuclear role in regulating DNA damage-induced apoptosis, which is distinct from its cytoplasmic role in activating NF-κB.

EXPERIMENTAL PROCEDURES

Cell Lines and Transfection—African green monkey kidney COS-7 cells and human osteosarcoma U2OS cells were maintained in Dulbecco's modified Eagle's medium, 10% fetal bovine serum, penicillin, and streptomycin (Invitrogen). Human lung carcinoma H1299, human neuroblastoma SK-N-AS, and mouse fibrosarcoma L929 cells were grown in RPMI 1640 medium, 10% fetal bovine serum, penicillin, and streptomycin. COS-7 cells were transfected with FuGENE 6 (Roche Applied Science) in accordance with the manufacturer's specifications. H1299 and U2OS cells were transfected with Lipofectamine (Invitrogen) according to the manufacturer's instructions. pcDNA3 (Invitrogen) was used as a blank plasmid to balance the amount of DNA introduced in transient transfection.

Cell Survival Assay—U2OS cells were seeded at 5×10^3/well in a 96-well tissue culture dish with 100 μl of complete medium and allowed to attach overnight. CDDP was added to the cultures at a final concentration of 20 μM, and cell viability was determined by a modified 3-(4,5-dimethylthiazol-2-yl)-2,5-diphenyltetrazolium bromide (MTT) assay at the indicated time points after the addition of CDDP as described (22).

RNA Extraction and Reverse Transcription (RT)-PCR—Total RNA was prepared from U2OS cells exposed to CDDP (20 μM) using an RNeasy mini kit (Qiagen Inc.) according to the manufacturer's protocol. For the RT-PCR, first-strand cDNA was generated using SuperScript II reverse transcriptase (Invitrogen) and random primers. PCR amplification was performed with r*Taq* DNA polymerase (Takara, Ohtsu, Japan).[3] The expression of glyceraldehyde-3-phosphate dehydrogenase was measured as an internal control.

Plasmids—The protein-coding region of IKK-α was amplified by PCR and inserted between the EcoRI and XhoI sites of pcDNA3-FLAG. The K44A mutation was introduced into wild-type IKK-α using PfuUltra™ high fidelity DNA polymerase (Stratagene) according to the manufacturer's instructions. The nucleotide sequence of the PCR product was determined to verify the presence of the desired mutation and the absence of random mutations.

Immunoblotting, Immunoprecipitation, and Glutathione S-Transferase (GST) Pulldown Assay—For immunoblotting, cell lysates (50 μg of protein) were analyzed using anti-FLAG monoclonal antibody M2 (Sigma); anti-hemagglutinin (HA) monoclonal antibody (12CA5, Roche Applied Biosciences); anti-p73 monoclonal antibody (Ab-4, NeoMarkers, Fremont, CA); anti-p53 monoclonal antibody (DO-1, Oncogene Research Products, Cambridge, MA); anti-Bax monoclonal antibody (6A7, eBioscience, San Diego, CA); anti-IKK-α polyclonal (M-280), anti-IKK-β polyclonal (H-470), anti-IKK-γ

[3] The list of primer sets used is available upon request.

polyclonal (FL-417), anti-p65 polyclonal (C-20), anti-IκB-α polyclonal (C-21), or polyclonal anti-$p21^{WAF1}$ (H-164) antibody (Santa Cruz Biotechnology, Inc., Santa Cruz, CA); or anti-actin polyclonal antibody (20–33, Sigma). After incubation with primary antibodies, membranes were incubated with horseradish peroxidase-conjugated secondary antibodies (Cell Signaling Technology, Beverly, MA), and immunoreactive proteins were finally visualized by the ECL system (Amersham Biosciences AB, Uppsala, Sweden). For immunoprecipitation, cell lysates were precleared with 30 μl of protein G-Sepharose suspension (Amersham Biosciences AB) and then incubated with anti-HA polyclonal antibody (Medical and Biological Laboratories, Nagoya, Japan) or anti-FLAG monoclonal antibody for 2 h at 4 °C. Immunoblotting was performed with anti-FLAG or anti-p73 monoclonal antibody as described above. For GST pulldown assay, [^{35}S]methionine-labeled FLAG-IKK-α was generated in the coupled transcription/translation system (Promega, Madison, WI) and mixed with GST or GST-p73 fusion proteins coupled to glutathione-Sepharose (Amersham Biosciences AB) for 2 h at 4 °C. ^{35}S-Labeled bound proteins were analyzed by 10% SDS-PAGE and visualized by autoradiography.

Subcellular Fractionation and Immunofluorescence Analysis—To prepare nuclear and cytoplasmic extracts, cells were lysed in 10 mM Tris-HCl (pH 7.5), 1 mM EDTA, 0.5% Nonidet P-40, 1 mM phenylmethylsulfonyl fluoride, and a protease inhibitor mixture (Sigma) and centrifuged at 5000 rpm for 10 min to collect soluble fractions, which are referred to as cytosolic extracts. Insoluble materials were washed with the lysis buffer and further dissolved in SDS sample buffer to collect the nuclear extracts. The nuclear and cytoplasmic fractions were subjected to immunoblot analysis using anti-lamin B monoclonal antibody (Ab-1; Oncogene Research Products) or anti-α-tubulin monoclonal antibody (DM1A, Cell Signaling Technology). For indirect immunofluorescence, U2OS cells were grown on coverslips and transfected with the indicated expression plasmids. Forty-eight hours after transfection, cells were fixed in 100% methanol for 20 min at −20 °C, blocked in 3% bovine serum albumin, stained with the corresponding antibodies, and examined with a laser scanning confocal microscope (Olympus, Tokyo, Japan). Nuclear matrix fractionation was performed as described previously (35, 36). In brief, cells were washed with ice-cold phosphate-buffered saline and lysed in 10 mM PIPES (pH 6.8), 100 mM NaCl, 300 mM sucrose, 3 mM $MgCl_2$, 1 mM EGTA, 1 mM dithiothreitol, and 0.5% Triton X-100 containing a protease inhibitor mixture, and insoluble materials were separated from soluble proteins (fraction I) by centrifugation. The pellet fraction was treated with DNase I (at a final concentration of 1 mg/ml) for 15 min at 37 °C, and then ammonium sulfate was added to the reaction mixture (at a final concentration of 0.25 M). The pellet fraction was separated from the supernatant (fraction II) by centrifugation and further extracted with 2 M NaCl (fraction III). The remaining pellet was solubilized in 8 M urea, 0.1 M NaH_2PO_4, and 10 mM Tris-HCl (pH 8.0) to give fraction IV.

Protein Stability and Ubiquitination Assays—COS-7 cells were transfected with HA-p73α with or without IKK-α. Cells were harvested at different time points after pretreatment with cycloheximide (100 μg/ml), and cell lysates were processed for immunoblot analysis with anti-p73 or anti-actin antibody. Densitometry was used to quantify the amounts of HA-p73α that normalized to actin. Ubiquitination assay was performed as described previously (37). COS-7 cells were cotransfected with HA-p73α and His-tagged ubiquitin with or without IKK-α. Forty hours after transfection, cells were exposed to the proteasomal inhibitor MG132 (20 μM) for 6 h. Cells were resuspended in 6 M guanidine HCl, 0.1 M Na_2HPO_4/NaH_2PO_4 (pH 8.0), and 10 mM imidazole, and ubiquitinated materials were recovered by nickel-nitrilotriacetic acid-agarose beads (Qiagen Inc.) and analyzed by immunoblotting with anti-HA antibody.

Luciferase Reporter and Apoptosis Assays—p53-deficient H1299 cells on 12-well plates were cotransfected with a p53/p73-responsive element-driven luciferase reporter, an internal control vector for *Renilla* luciferase, and a combination of the indicated expression vectors. Both firefly and *Renilla* luciferase activities were assayed with the Dual-Luciferase reporter assay system (Promega). The firefly luminescence signal was normalized based on the *Renilla* luminescence signal. For apoptosis assay, H1299 cells on 6-well plates were cotransfected with β-galactosidase (50 ng) and HA-p73α (50 ng) with or without increasing amounts of IKK-α or IKK-β (100, 200, and 400 ng). Forty-eight hours after transfection, cells were stained with a 0.4% solution of trypan blue for 10 min at room temperature. Thereafter, cells were fixed in phosphate-buffered saline containing 2.5% glutaraldehyde, 1 mM $MgCl_2$, and 2 mM EGTA for 10 min and then stained with Red-Gal for 2 h as described (11). Red-Gal was used as a marker to visualize the transfected cells and to assess the apoptotic frequency among the transfectants. Apoptotic cells were scored by rounding up of cells with dark pink-purple coloration due to double staining with Red-Gal and trypan blue.

In Vitro Kinase Assay—GST or GST-p73 deletion mutants were incubated with the active form of IKK-α (Upstate Biotechnology, Lake Placid, NY) in a solution containing 40 mM MOPS-NaOH (pH 7.0), 1 mM EDTA, 25 mM sodium acetate, and 0.25 mM ATP in the presence of [γ-^{32}P]ATP at 30 °C for 10 min. After incubation, the reaction mixtures were separated by SDS-PAGE. The gel was then dried and subjected to autoradiography.

RNA Interference—To knock down endogenous IKK-α, the expression plasmid for siRNA directed against human IKK-α (GeneSuppressor, Imgenex Corp., San Diego, CA) was introduced into U2OS cells using Lipofectamine following the manufacturer's instructions. Forty-eight hours after transfection, whole cell lysates were prepared and analyzed for the expression levels of IKK-α by immunoblotting.

Chromatin Immunoprecipitation Assays—Chromatin immunoprecipitation assays were performed following a protocol provided by Upstate Biotechnology (Lake Placid, NY). In brief, cells were cross-linked with 1% formaldehyde in medium for 10 min at 37 °C. Chromatin solutions were prepared and immunoprecipitated with anti-HA antibody. DNAs of the immunoprecipitates and control input DNAs were purified using a QIAquick PCR purification kit (Qiagen Inc.) and then analyzed by regular PCR using human *Bax* promoter-specific

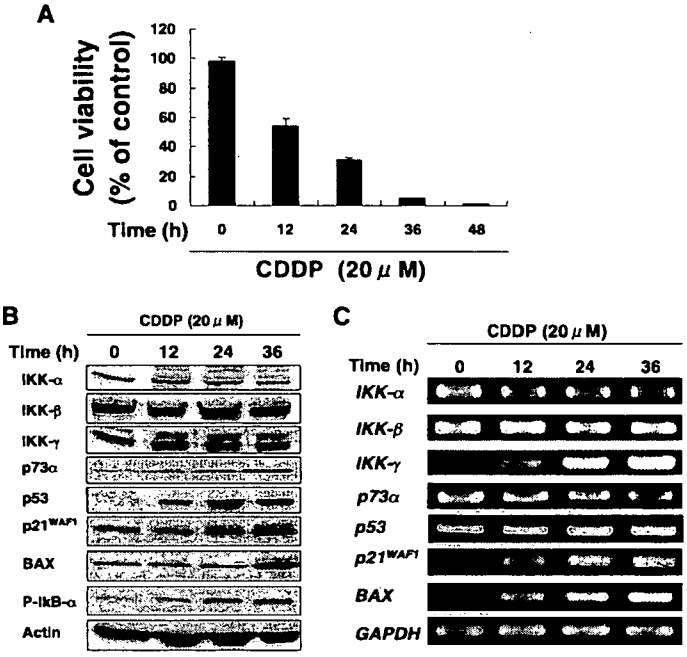

FIGURE 1. **Induction of IKK-α in response to CDDP.** *A*, effect of CDDP on osteosarcoma-derived U2OS cell survival. At the indicated time points after treatment with CDDP (at a final concentration of 20 μM), cell viability was determined by MTT assays. *B*, immunoblot analysis. At the indicated time periods after treatment with CDDP, whole cell lysates were prepared and subjected to immunoblotting with the indicated antibodies. For p73α, whole cell lysates were subjected to immunoprecipitation with anti-p73 antibody, followed by immunoblotting with anti-p73 antibody. Actin expression served as a control for equal loading of proteins in each lane. *C*, RT-PCR analysis. Total RNA was extracted from U2OS cells at the indicated times after CDDP treatment and used for RT-PCR with the indicated primers. Glyceraldehyde-3-phosphate dehydrogenase (*GAPDH*) was used as a control.

primers. The primer sequences used were 5′-AGGCTGAGACG-GGGTTATCT-3′ and 5′-AAAGCTCAGAGGCCCAAAAT-3′.

RESULTS

Induction of IKK-α during CDDP-mediated Apoptosis in U2OS Cells—To define the potential function(s) of IKKs in DNA damage-induced signaling, we first examined their expression levels in human osteosarcoma-derived U2OS cells exposed to the DNA-damaging chemotherapeutic drug CDDP. Under our experimental conditions, U2OS cells underwent apoptosis in a time-dependent manner as examined by cell survival assays (Fig. 1*A*). Similar results were also obtained by fluorescence-activated cell sorter analysis (data not shown). Immunoblot analysis demonstrated that p53 and its homolog p73α, which are major mediators in the DNA damage response (reviewed in Refs. 14 and 38), were significantly induced at protein levels in response to CDDP (Fig. 1*B*), whereas the expression of *p53* and *p73α* mRNAs remained unchanged (Fig. 1*C*). Their accumulation was associated with several of their downstream effectors, including $p21^{WAF1}$ and Bax. Notably, CDDP treatment led to a remarkable accumulation of IKK-α, and its induction was observed between 12 and 36 h after exposure to CDDP (Fig. 1*B*). Twelve hours after treatment with CDDP, the amount of IKK-γ (NEMO) was transiently increased at the protein level. By contrast, the amount of IKK-β was not significantly altered upon CDDP treatment.

RT-PCR analysis revealed that the expression levels of *IKK-α* and *IKK-β* mRNAs remained unchanged regardless of CDDP treatment, whereas a marked increase in the expression level of *IKK-γ* mRNA was detected in a time-dependent manner in response to CDDP (Fig. 1*C*). Intriguingly, immunoblot analysis also demonstrated that CDDP treatment caused a significant increase in the phosphorylated form of IκB-α, which is a well characterized substrate for the IKK complex (reviewed in Ref. 3). Taken together, these results suggest that DNA damage-induced accumulation of both p53 and p73α is associated with the up-regulation of IKK-α and IKK-γ and that a functional interaction might exist between them in DNA damage-mediated apoptotic pathways.

Nuclear Accumulation of IKK-α in Response to CDDP—It was shown recently that IKK-α shuttles between the nucleus and cytoplasm in a CRM1-dependent fashion (32). Nuclear IKK-α has the ability to transactivate NF-κB-responsive genes that control survival pathways after cytokine exposure (33, 34). In addition, Verma *et al.* (39) found that, like IKK-α, IKK-γ is present in both the nucleus and cytoplasm. These observations prompted us to examine whether the subcellular localization of endogenous IKKs can change in response to CDDP. For this purpose, nuclear and cytoplasmic extracts were prepared from U2OS cells exposed to CDDP or left untreated and then subjected to immunoblotting with the indicated antibodies. In agreement with previous results (33), IKK-α was localized in both the nucleus and cytoplasm, whereas IKK-β was expressed almost exclusively in the cytoplasm (Fig. 2*A*). The amounts of cytoplasmic IKK-α, IKK-β, and IKK-γ remained unchanged regardless of the treatment with CDDP. Of note, CDDP treatment led to a remarkable accumulation of IKK-α in the cell nucleus in a time-dependent manner, whereas IKK-β accumulated in the cell nucleus to a lesser degree. The temporal patterns of CDDP-mediated accumulation of nuclear IKK-α correlated with those of p73α. On the other hand, the transient nuclear accumulation of IKK-γ was detected 12 h after exposure to CDDP. Compared with the levels of nuclear IKK-α accumulated in response to CDDP, the amount of nuclear IKK-γ was small. Consistent with the enhanced phosphorylation of IκB-α in response to CDDP, cytoplasmic IκB-α was decreased in a time-dependent manner. However, CDDP treatment had little or no effect on the nuclear accumulation of the NF-κB p65 subunit (RelA), indicating that nuclear translocation of p65 might be inhibited in the presence of CDDP. Considering that, among IKKs, CDDP treatment promoted a significant nuclear accumulation of IKK-α, it is likely that IKK-α might have a certain nuclear function during CDDP-mediated apoptosis.

To investigate whether exogenously expressed IKK-α can reflect the behavior of endogenous IKK-α, we examined the intracellular distribution of exogenous IKK-α by immunoblotting and immunofluorescence staining. Nuclear and cytoplasmic fractions were prepared from U2OS cells transfected with the expression plasmid for FLAG-IKK-α or HA-p73α and subjected to immunoblotting with anti-FLAG or anti-p73α antibody, respectively. As shown in Fig. 2*B*, HA-p73α was localized exclusively in the cell nucleus, whereas FLAG-IKK-α was present in both the nucleus and cytoplasm. Surprisingly, immunofluorescence staining with anti-FLAG and anti-lamin B antibodies clearly showed that exogenous IKK-α was localized in

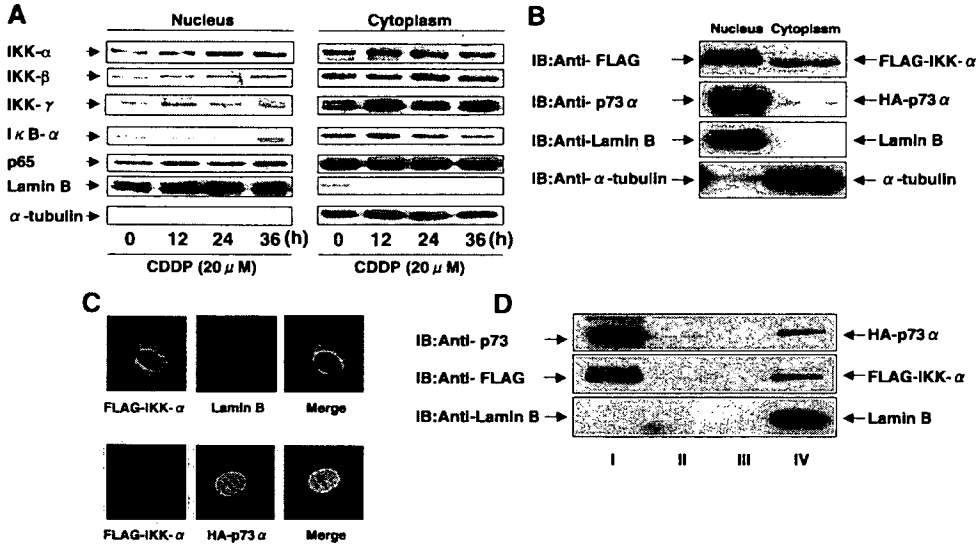

FIGURE 2. **Nuclear accumulation of IKK-α.** *A*, nuclear accumulation of IKK-α in response to CDDP. At the indicated time periods after the addition of CDDP, U2OS cells were fractionated into nuclear and cytoplasmic fractions and then analyzed by immunoblotting with the indicated antibodies. Anti-lamin B and anti-α-tubulin immunoblotting were included to assess the purity of each fraction. *B*, subcellular localization of exogenous IKK-α. U2OS cells were transiently transfected with the expression plasmid for FLAG-IKK-α or HA-p73α. Cells were subjected to biochemical fractionation, followed by immunoblotting (*IB*) with anti-FLAG or anti-p73 antibody. *C*, co-localization of IKK-α and p73 in nuclear laminae. U2OS cells were transiently transfected with the FLAG-IKK-α expression plasmid alone (*upper panels*) or with the HA-p73α expression plasmid (*lower panels*). Cells were processed for indirect immunofluorescence and double-stained with anti-FLAG and anti-lamin B antibodies (*upper panels*) or with anti-HA and anti-FLAG antibodies (*lower panels*). The merged images show that IKK-α co-localized with p73α in nuclear laminae (*yellow*). *D*, p73α and IKK-α are detected in the nuclear matrix fraction. U2OS cells cotransfected with the expression plasmids for HA-p73α and FLAG-IKK-α were subjected to high salt nuclear matrix fractionation as described under "Experimental Procedures." Each fraction was analyzed by immunoblotting with anti-p73 (*upper panel*), anti-IKK-α (*middle panel*), or anti-lamin B (*lower panel*) antibody.

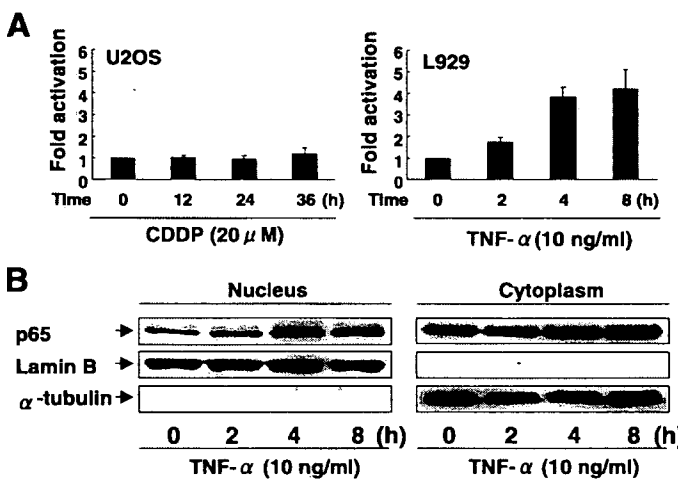

FIGURE 3. **NF-κB is not activated in response to CDDP.** *A*, U2OS (*left panel*) or L929 (*right panel*) cells were cotransfected with the NF-κB reporter construct (pELAM1-Luc) and the *Renilla* luciferase plasmid (pRL-tk). Twenty-four hours after transfection, U2OS and L929 cells were treated with CDDP and TNF-α, respectively. At the indicated time points after treatment, luciferase activity was determined. *B*, nuclear accumulation of p65 in L929 cells exposed to TNF-α. At the indicated time periods after treatment with TNF-α, L929 cells were fractionated into nuclear and cytoplasmic fractions and then analyzed directly by immunoblotting with anti-p65 antibody.

the cytoplasm and nuclear lamina, as indicated by the extensive co-localization with lamin B, a nuclear lamina marker (Fig. 2*C*). Intriguingly, HA-p73α was co-localized with FLAG-IKK-α in the nuclear lamina of the transfected cells. To confirm these observations, nuclear matrix fractionation was performed 48 h after transfection, and the fractions obtained were subjected to immunoblotting. As shown in Fig. 2*D*, HA-p73α and FLAG-IKK-α were detected in nuclear matrix fraction (fraction IV). Our results suggest that nuclear IKK-α might interact with pro-apoptotic p73α and modulate its function.

As described above, the amounts of the nuclear transactivating p65 subunit remained unchanged in U2OS cells treated with CDDP. These findings prompted us to examine whether NF-κB activation can be detected in response to CDDP. To this end, U2OS cells transfected with the NF-κB reporter plasmid (40) were treated with CDDP, and their luciferase activity was determined. Consistent with the previous observations (13), CDDP treatment did not enhance NF-κB-dependent transcriptional activation (Fig. 3*A*, *left panel*). Under our experimental conditions, NF-κB-dependent transcriptional activation was detected within 2 h of exposure to TNF-α in the mouse fibrosarcoma cell line L929 (Fig. 3*A*, *right panel*), which is widely used to investigate TNF-α-dependent NF-κB activation (41). In addition, treatment of L929 cells with TNF-α caused a nuclear accumulation of p65 (Fig. 3*B*). Thus, it is likely that, the lack of a significant effect of CDDP on NF-κB-dependent transcriptional activation could be attributed to lack of the regulated nuclear accumulation of p65.

IKK-α Interacts with p73—To determine whether IKK-α can interact with p73 in cells, whole cell lysates prepared from transfected COS-7 cells were immunoprecipitated with anti-FLAG or anti-HA antibody and analyzed by immunoblotting using anti-p73 or anti-FLAG antibody, respectively. As shown in Fig. 4*A*, exogenously expressed FLAG-IKK-α and HA-p73α formed stable complexes in COS-7 cells. Similarly, HA-p73β was co-immunoprecipitated with FLAG-IKK-α (data not shown). Their interaction was further examined using endogenous materials. As shown in Fig. 4*B*, endogenous p73α formed a protein complex with endogenous IKK-α in U2OS cells exposed to CDDP. Similar results were also obtained in HeLa cells (data not shown). In contrast, immunoprecipitation of endogenous p53 followed by immunoblotting with anti-FLAG antibody did not detect co-immunoprecipitated FLAG-IKK-α (Fig. 4*C*), indicating that IKK-α interacts with p73, but not with p53, in cells. To identify the p73 determinants involved in the interaction with IKK-α, we generated several deletion mutants of p73α fused to GST and tested their ability to bind to FLAG-IKK-α in GST pulldown assays. These mutants were designed based on p73α, including the transactivation, DNA-binding,

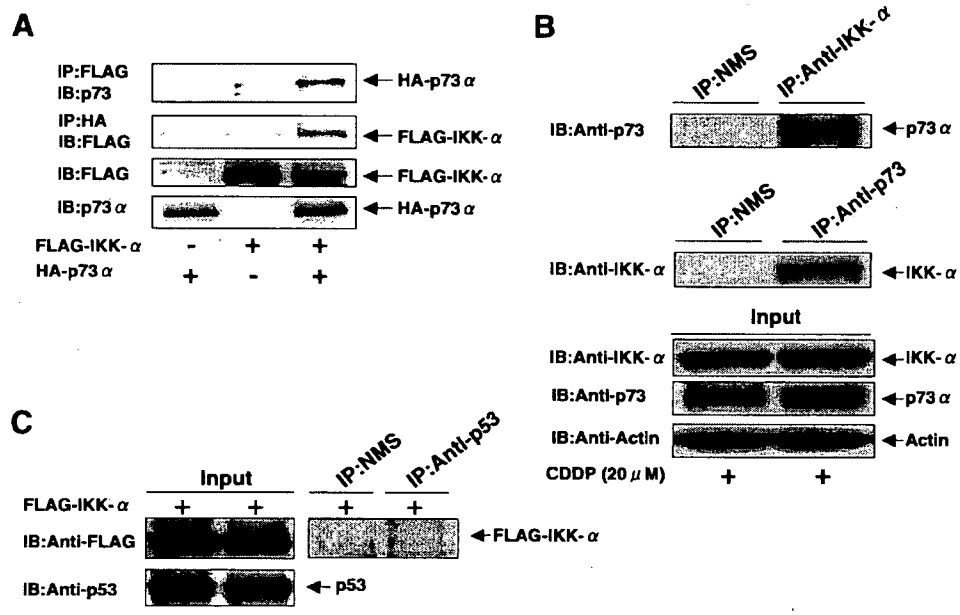

FIGURE 4. **Interaction between IKK-α and p73α.** *A*, FLAG-IKK-α was transiently coexpressed with HA-p73α in COS-7 cells as indicated. Whole cell lysates were subjected to immunoprecipitation (*IP*) with anti-FLAG or anti-HA antibody, followed by immunoblotting (*IB*) with anti-p73 or anti-FLAG antibody, respectively. *B*, whole cell lysates were prepared from U2OS cells exposed to CDDP and subjected to immunoprecipitation with normal mouse serum (*NMS*), anti-IKK-α antibody, or anti-p73 antibody, followed by immunoblotting with the indicated antibodies. *C*, FLAG-IKK-α was transiently transfected into COS-7 cells. Whole cell lysates were subjected to immunoprecipitation with normal mouse serum or anti-p53 antibody, followed by immunoblotting with anti-FLAG antibody. *Input* represents the 10% materials used for immunoprecipitation in *B* and *C*.

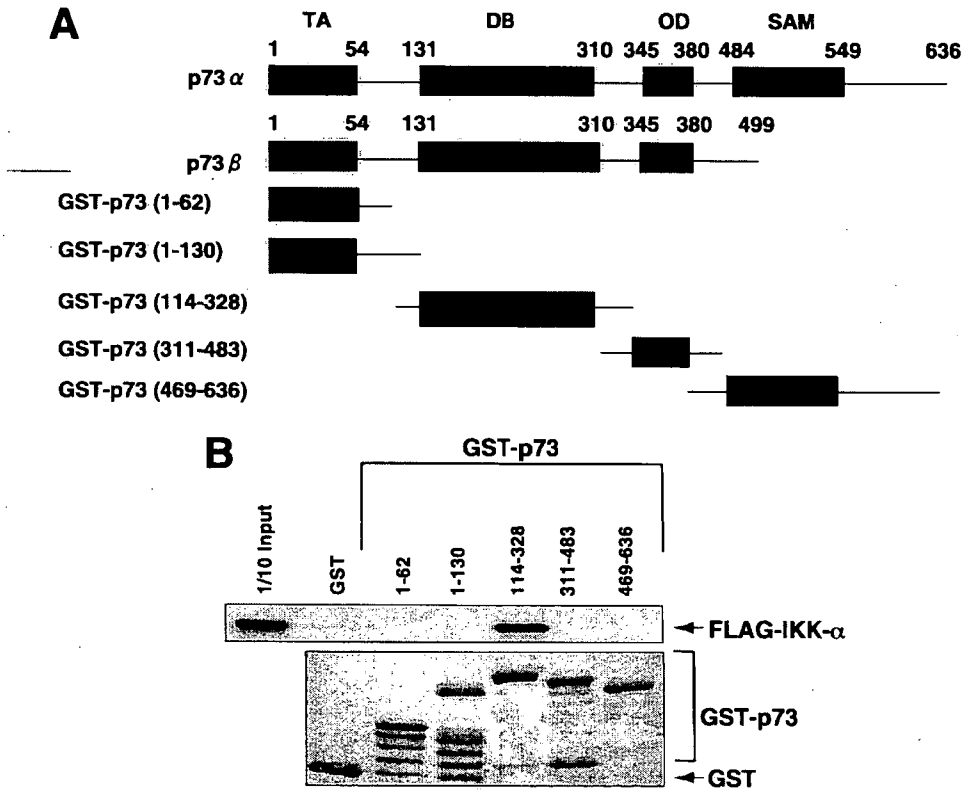

FIGURE 5. **DNA-binding domain of p73α is required for interaction with IKK-α.** *A*, shown is a schematic representation of the GST-p73 fusion proteins. *TA*, transactivation domain; *DB*, DNA-binding domain; *OD*, oligomerization domain; *SAM*, sterile α-motif domain. *B*, the DNA-binding domain of p73α is required for the interaction with IKK-α. ^{35}S-Labeled FLAG-IKK-α was incubated with GST or the indicated GST-p73 fusion proteins, and bound radiolabeled proteins were recovered on glutathione-Sepharose beads and visualized by autoradiography. The 1/10 volumes of input sample (*1/10 Input*) of ^{35}S-labeled FLAG-IKK-α used for pulldown assay were applied to the same gel (*upper panel*). Coomassie Blue-stained GST-p73 fusion proteins together with GST are also shown (*lower panel*).

oligomerization, and sterile α-motif domains (Fig. 5*A*). As shown in Fig. 5*B*, radiolabeled FLAG-IKK-α bound to GST-p73-(114–328), but not to the other GST fusion proteins. Taken together, our results suggest that IKK-α directly interacts with p73 through its DNA-binding domain.

IKK-α Increases p73 Stability—As described previously (16, 42), some p73-interacting protein kinases, including c-Abl and protein kinase Cδ, can stabilize p73. To investigate whether IKK-α can affect the stability of p73, COS-7 cells were transiently cotransfected with equal amounts of the HA-p73α expression plasmid with or without increasing amounts of the expression plasmid encoding IKK-α, and the protein level of HA-p73α was examined. As shown in Fig. 6*A*, the amount of HA-p73α was significantly increased in the presence of exogenous IKK-α, whereas IKK-α had no detectable impact on the stability of FLAG-p53. In addition, HA-p73β was also stabilized by IKK-α, but to a lesser degree compared with HA-p73α. *p73α* mRNA levels remained unchanged in the presence of IKK-α (Fig. 6*A*, *lower panels*), suggesting that IKK-α regulates p73 at the protein level. Next, we examined the possible effect of IKK-β on the stability of p73 and p53 by transient cotransfection. As shown in Fig. 6*B*, FLAG-IKK-β had negligible effects on the stability of both p73α and p53.

To investigate a possible role of endogenous IKK-α in the regulation of p73 stability, we employed RNA interference to block IKK-α expression. The enforced expression of siRNA against IKK-α in U2OS cells resulted in a significant reduction of endogenous IKK-α (Fig. 6*C*). We then tested the effect of knockdown of endogenous IKK-α on the CDDP-mediated accumulation of p73α. U2OS cells were transiently transfected with the expression plasmid for siRNA against IKK-α and exposed to CDDP for 36 h. As shown in Fig. 6*C*, down-regulation of endogenous IKK-α expression

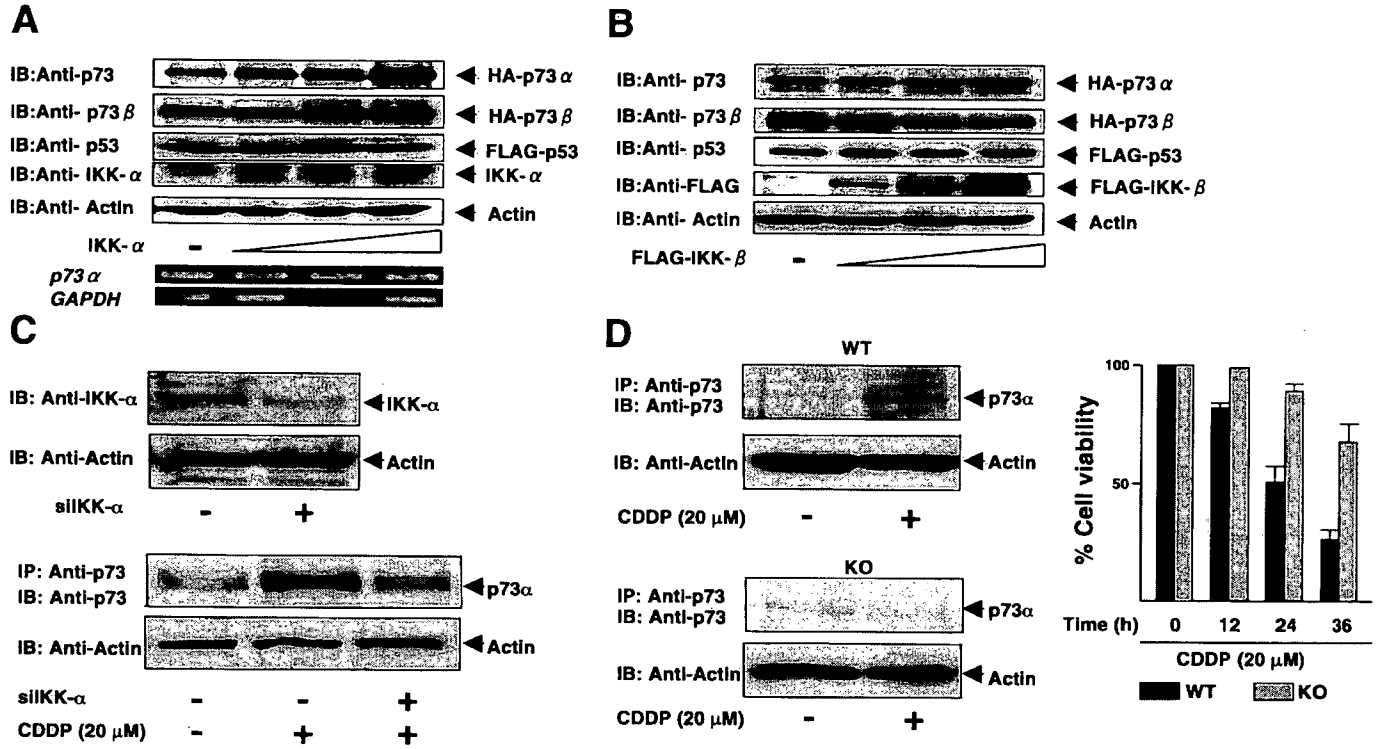

FIGURE 6. **IKK-α increases p73α stability.** *A*, the ectopic expression of IKK-α increases the stability of p73, but not of p53. COS-7 cells were transiently cotransfected with the indicated combinations of expression plasmids. Whole cell lysates and total RNA were prepared and subjected to immunoblotting (*IB*) (*upper panels*) or RT-PCR (*lower panels*), respectively. *GAPDH*, glyceraldehyde-3-phosphate dehydrogenase. *B*, IKK-β does not affect the stability of p73. COS-7 cells were transiently cotransfected with the indicated combinations of expression plasmids. Whole cell lysates were subjected to immunoblotting with the indicated antibodies. *C*, the reduction of endogenous IKK-α results in the attenuation of the CDDP-mediated accumulation of p73α. U2OS cells were transiently transfected with the expression plasmid for siRNA against IKK-α (*siIKK-α*) or with the scrambled control. Forty-eight hours after transfection, whole cell lysates were analyzed by immunoblotting with anti-IKK-α antibody. *Upper panels*, actin levels were used to monitor loading. *Lower panels*, U2OS cells were transiently transfected with the expression plasmid as in the *upper panels*. Twenty-four hours after transfection, cells were exposed to CDDP (at a final concentration of 20 μM) for 36 h or left untreated. Equal amounts of whole cell lysates were subjected to immunoprecipitation with anti-p73 antibody, followed by immunoblotting with anti-p73 antibody. Actin was included as a loading control. *D*, the CDDP-mediated accumulation of p73α is not detectable in IKK-$\alpha^{-/-}$ MEFs. Wild-type (*WT*) and IKK-$\alpha^{-/-}$ MEFs were treated with or without CDDP (at a final concentration of 20 μM) for 24 h. Equal amounts of whole cell lysates were subjected to immunoprecipitation (*IP*) with anti-p73 antibody, followed by immunoblotting with anti-p73 antibody. *Left panels*, actin was included as a loading control. *Right panel*, shown are the results of MTT assay. Wild-type and IKK-$\alpha^{-/-}$ MEFs were treated with CDDP (at a final concentration of 20 μM). At the indicated time periods after CDDP treatment, their viability was examined by MTT assay. *KO*, knock-out.

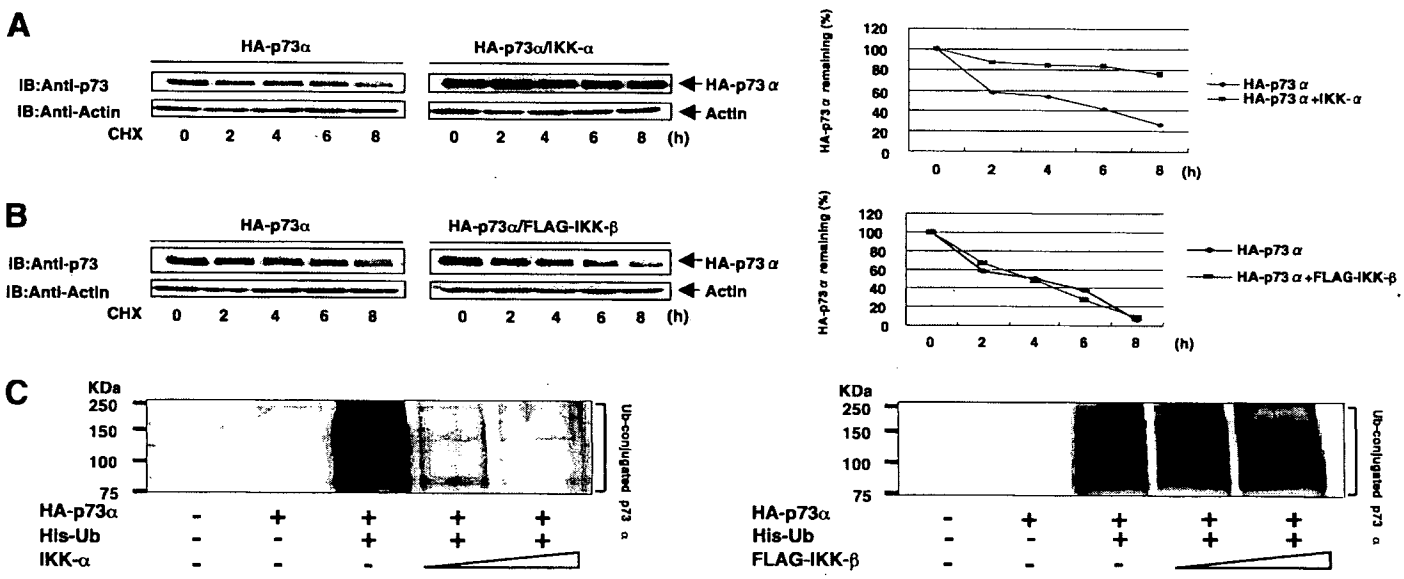

FIGURE 7. **IKK-α increases the half-life of p73α.** *A* and *B*, IKK-α or the FLAG-IKK-β expression plasmid, respectively, was transiently transfected into COS-7 cells with the expression plasmid for HA-p73α for 24 h. Cells were treated with cycloheximide (*CHX*) and harvested at the indicated time periods, followed by immunoblotting (*IB*) with anti-p73 antibody. The intensity of the bands was quantified by densitometry, and the HA-p73α remaining is indicated graphically. *C*, IKK-α inhibits the ubiquitination of p73. COS-7 cells were transiently cotransfected with the indicated combinations of expression plasmids and treated with MG132. Ubiquitinated products were recovered on nickel-agarose beads and separated by SDS-PAGE, followed by immunoblotting with anti-HA antibody. The *brackets* indicate slowly migrating ubiquitinated (*Ub*) forms of HA-p73α.

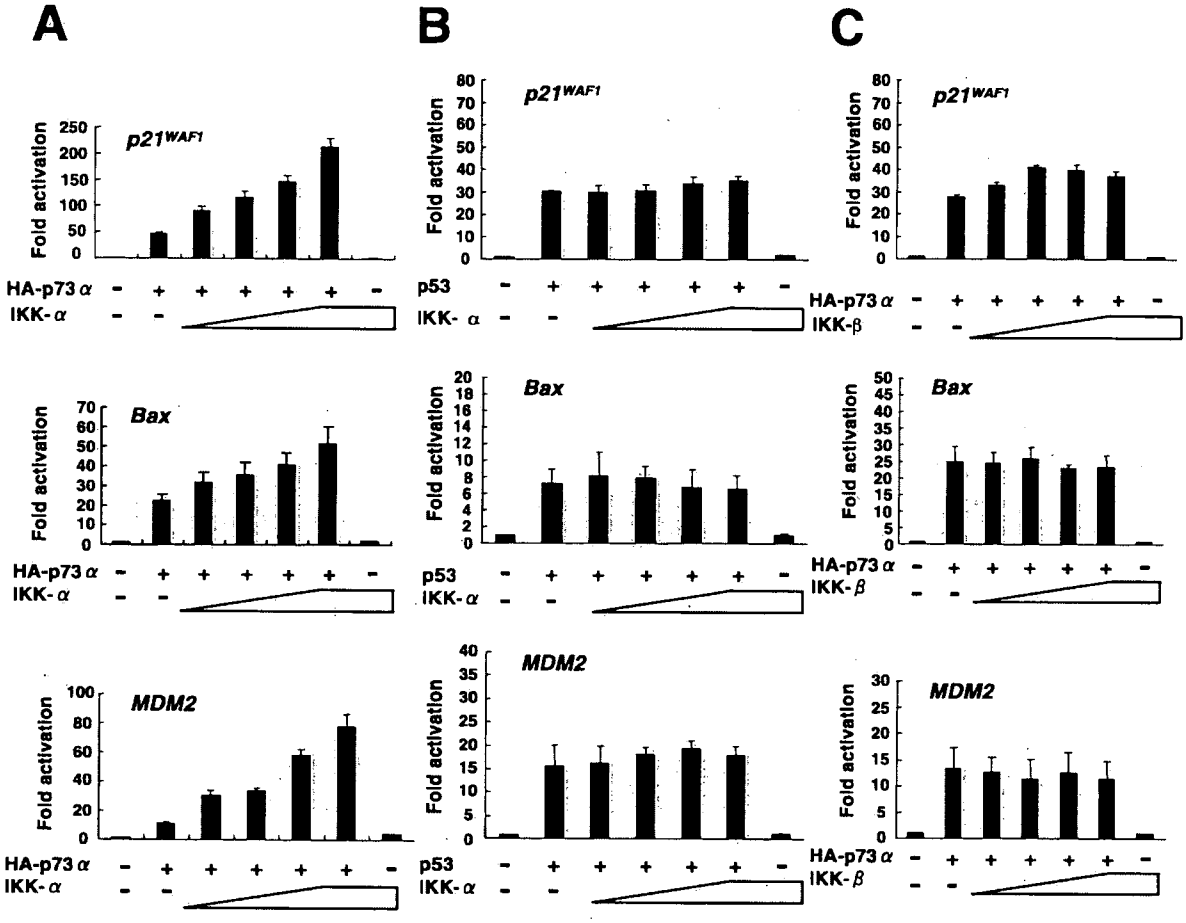
A
B
C
p21WAF1
Bax
MDM2
Fold activation
HA-p73α
IKK-α
IKK-β
p53

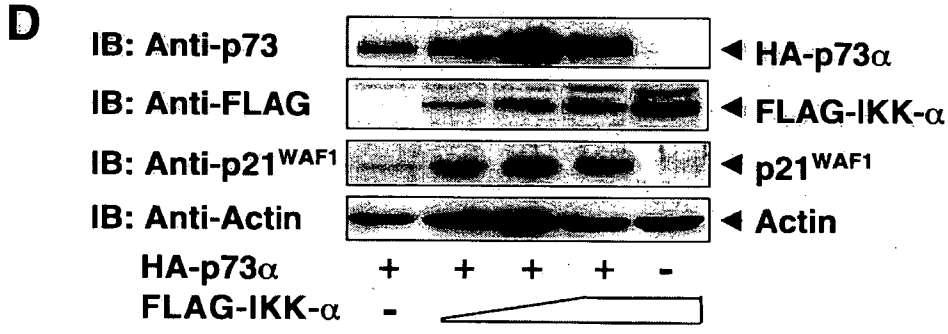
D
IB: Anti-p73
IB: Anti-FLAG
IB: Anti-p21WAF1
IB: Anti-Actin
HA-p73α
FLAG-IKK-α
Actin

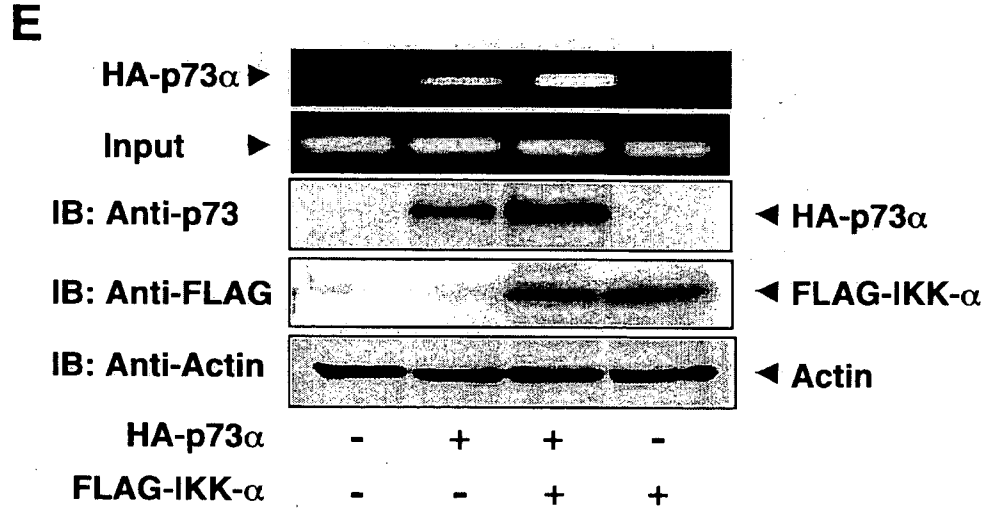
E
HA-p73α
Input
IB: Anti-p73
IB: Anti-FLAG
IB: Anti-Actin
FLAG-IKK-α
Actin

markedly inhibited the CDDP-mediated accumulation of p73α. To further confirm the effects of endogenous IKK-α, wild-type and IKK-$\alpha^{-/-}$ MEFs were treated with or without CDDP for 24 h, and whole cell lysates were immunoprecipitated with anti-p73 antibody. As expected, CDDP-mediated accumulation of endogenous p73α was detected in wild-type, but not IKK-$\alpha^{-/-}$, MEFs, and CDDP sensitivity was decreased in IKK-$\alpha^{-/-}$ MEFs compared with wild-type MEFs (Fig. 6*D*).

To explore whether IKK-α can modulate p73 turnover, we examined the decay rate of p73α in COS-7 cells. Twenty-four hours after transfection, cells were treated with cycloheximide. At the indicated time points, whole cell lysates were prepared and subjected to immunoblotting with anti-p73 antibody. As shown in Fig. 7*A*, the degradation rate of HA-p73α was slower in cells expressing both HA-p73α and IKK-α than that in cells expressing HA-p73α alone. In contrast, the half-life of HA-p73α was not prolonged in the presence of FLAG-IKK-β (Fig. 7*B*). An IKK-α-mediated increase in the half-life of endogenous p73α was also observed. Thus, IKK-α-mediated p73α stabilization resulted from the increase in the half-life of p73α. As described previously (43), the steady-state level of p73 is regulated at least in part by the protein degradation process through the ubiquitin/proteasome pathway. We then determined whether IKK-α can inhibit the ubiquitination of p73. To this end, COS-7 cells were transiently cotransfected with the expression plasmids for HA-p73α and His-ubiquitin with or without increasing amounts of the expression plasmid for IKK-α or FLAG-IKK-β. Forty-eight hours after transfection, whole cell lysates were prepared and analyzed by immunoblotting for the presence of His-ubiquitin-containing p73α. As shown in Fig. 7*C*, the amounts of the ubiquitinated forms of p73α were decreased in the presence of IKK-α, whereas FLAG-IKK-β inhibited the ubiquitination of p73α to a lesser degree. Taken together, these results strongly suggest that IKK-α inhibits the ubiquitination of p73α, thereby increasing the stability of p73α.

IKK-α Enhances p73-mediated Transactivation and Pro-apoptotic Functions in p53-deficient H1299 Cells—To address the functional implications of the interaction between IKK-α and p73, we first examined the effects of IKK-α on p73-mediated transcriptional activation. To this end, we cotransfected p53-deficient H1299 cells with the HA-p73α expression plasmid and the luciferase reporter construct under the control of the $p21^{WAF1}$, *bax*, or *MDM2* promoter with or without increasing amounts of the expression plasmid encoding IKK-α. As shown in Fig. 8*A*, ectopically expressed p73α successfully activated the transcription of each of these p53/p73-responsive reporters compared with the empty control plasmids, and IKK-α alone had little effect on luciferase activity. When HA-p73α was coexpressed with IKK-α, a marked increase in p73α-dependent transcriptional activation was observed in a dose-dependent manner. IKK-α also enhanced p73β-mediated transcriptional activation (data not shown). In contrast, there was no detectable IKK-α-induced increase in p53-dependent reporter gene activity (Fig. 8*B*). To examine the specificity of the IKK-α-mediated activation of p73-dependent transcription, we investigated whether IKK-β can enhance p73 transcriptional activity for the p53/p73-responsive promoters. As shown in Fig. 8*C*, no significant changes in p73α-dependent transcriptional activation were found with FLAG-IKK-β. In addition, the ectopic expression of IKK-α had no detectable effects on luciferase activity in p73-deficient neuroblastoma SK-N-AS cells bearing a mutant form of p53 (15, 44). Furthermore, the exogenous expression of IKK-α in H1299 cells resulted in a significant up-regulation of the p73α-mediated induction of endogenous $p21^{WAF1}$ (Fig. 8*D*). To address whether the amounts of p73α associated with the p53/p73-responsive promoter can be increased in the presence of exogenous IKK-α, H1299 cells were transiently cotransfected with the expression plasmid for HA-p73α with or without the FLAG-IKK-α expression plasmid and subjected to chromatin immunoprecipitation analysis. As shown in Fig. 8*E*, the IKK-α-inducible association of p73α with the *bax* promoter was detected. Taken together, these results strongly suggest that IKK-α specifically enhances the transcriptional activity of p73.

We next investigated the potential impact of IKK-α on p73-dependent biological functions such as the regulation of apoptosis. H1299 cells were transiently cotransfected with a constant amount of HA-p73α and β-galactosidase expression plasmids with or without increasing amounts of the expression plasmid for IKK-α or FLAG-IKK-β. The β-galactosidase expression plasmid was used to identify the transfected cells. Forty-eight hours after transfection, cells were subjected to double staining with trypan blue (nonviable cells) and Red-Gal (transfected cells), and the number of cells with purple coloration was scored as described previously (11). As shown in Fig. 9 (*A* and *B*), the coexpression of IKK-α with HA-p73α resulted in an increase in the number of apoptotic cells compared with the expression of HA-p73α alone. In contrast, the coexpression of FLAG-IKK-β had no significant effect on p73α-dependent apoptosis (Fig. 9*C*). These data are consistent with the positive effect of IKK-α on p73-dependent transcriptional activation.

Kinase-deficient Mutant IKK-α Fails to Stabilize p73—To examine whether the intrinsic kinase activity of IKK-α is required for the stabilization of p73, we generated a mutant form of IKK-α (IKK-α(K44A)) in which Lys^{44} within the ATP-binding motif was replaced with Ala. As described previously (45), mutation of this site impairs the kinase activity of IKK-α.

FIGURE 8. **IKK-α enhances the transcriptional activity of p73α.** *A* and *B*, p53-deficient H1299 cells were transiently cotransfected with the expression plasmid for HA-p73α or p53, respectively, with the indicated p53/p73 luciferase reporter construct in the presence or absence of the IKK-α expression plasmid, followed by reporter assay. *C*, IKK-β does not affect p73-mediated transcriptional activation. H1299 cells were transiently cotransfected with the expression plasmid encoding HA-p73α and the indicated reporter constructs with or without the IKK-β expression plasmid, followed by reporter assay. *D*, shown are the results from analysis of endogenous $p21^{WAF1}$. H1299 cells were transiently cotransfected with the indicated expression plasmids. Whole cell lysates were subjected to immunoblotting (*IB*) with the indicated antibodies. *E*, IKK-α increases the amount of p73α associated with the human *bax* promoter. H1299 cells were transiently cotransfected with the indicated combinations of expression plasmids. Forty-eight hours after transfection, cells were cross-linked with 1% formaldehyde and subjected to chromatin immunoprecipitation assays, followed by PCR analysis as described under "Experimental Procedures" (*upper panels*). Immunoblotting of the indicated proteins is also shown (*lower panels*).

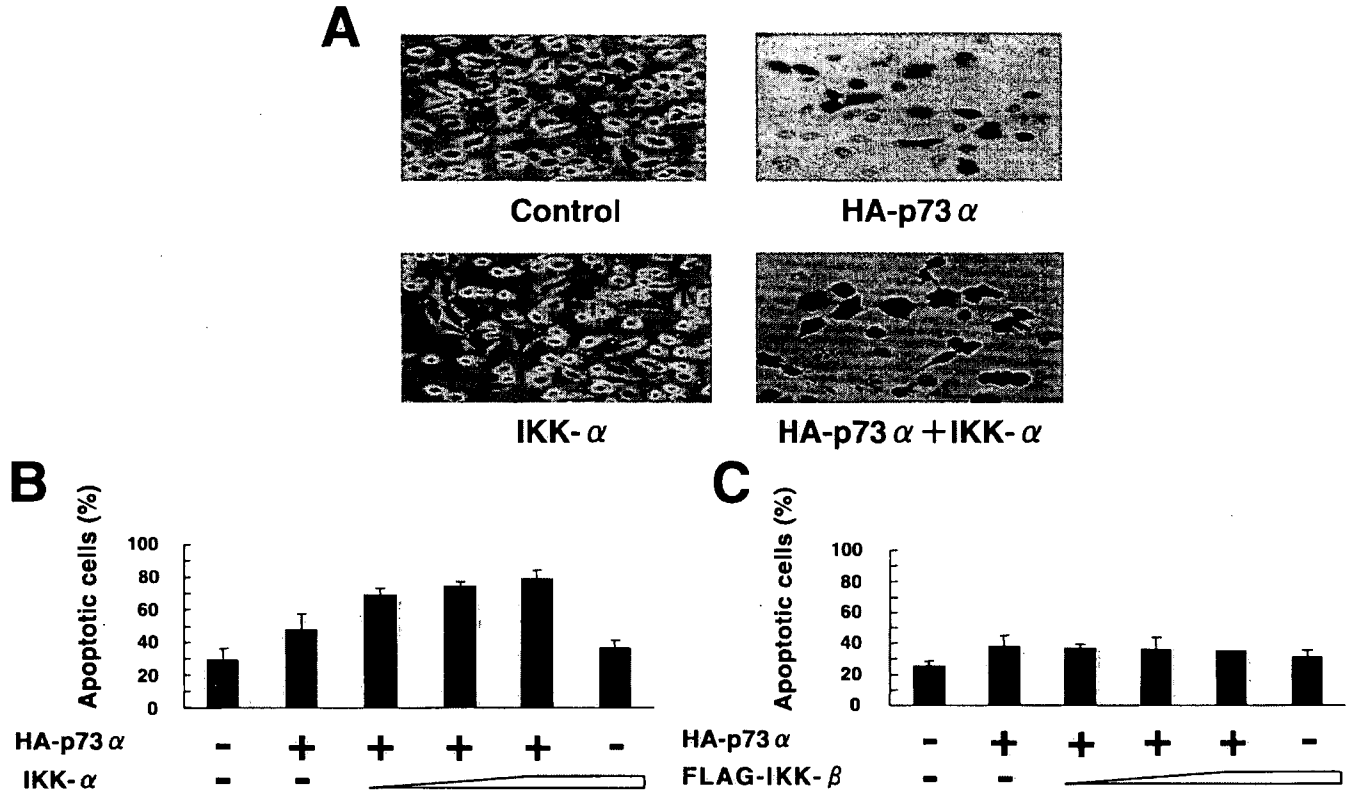

FIGURE 9. **IKK-α enhances the pro-apoptotic function of p73α.** *A* and *B*, H1299 cells were transiently cotransfected with the expression plasmids for HA-p73α and β-galactosidase with or without IKK-α. Control transfection was performed with the empty plasmid plus the β-galactosidase expression plasmid. Forty-eight hours after transfection, cells were double-stained with trypan blue (*blue*) and Red-Gal (*red*) (*A*), and the number of transfected cells (positive for β-galactosidase) and transfected apoptotic cells (*dark pink-purple*) in at least three different fields (>300 transfected cells) was measured. The percentage of transfected apoptotic cells is indicated (*B*). *C*, H1299 cells were transiently cotransfected with the indicated combinations of expression plasmids plus the β-galactosidase expression plasmid and processed for double staining as described above. The percentage of transfected apoptotic cells is indicated.

Immunoprecipitation analysis indicated that IKK-α(K44A) retained the ability to form a complex with p73α in cells (Fig. 10*A*). In sharp contrast to wild-type IKK-α, the coexpression of FLAG-IKK-α(K44A) had little or no effect on the intracellular level of exogenously expressed HA-p73α (Fig. 10*B*). To examine the effect of kinase-deficient IKK-α on endogenous p73, U2OS cells were transiently transfected with the empty plasmid or the FLAG-IKK-α(K44A) expression plasmid and then exposed to CDDP for 24 h or left untreated. Whole cell lysates and total RNA were prepared and subjected to immunoblotting and RT-PCR, respectively. As shown in Fig. 10*C*, the CDDP-mediated stabilization of endogenous p73α was markedly inhibited in U2OS cells transfected with the FLAG-IKK-α(K44A) expression plasmid, whereas FLAG-IKK-α(K44A) had no significant effect on the amount of endogenous p53. In good agreement with the observations above, CDDP-induced apoptosis was significantly inhibited in the presence of FLAG-IKK-α(K44A) (Fig. 10*D*). Similar results were also obtained in H1299 cells (Fig. 10, *E* and *F*). Thus, the kinase activity of IKK-α appears to be required for the stabilization of p73 in response to CDDP-induced DNA damage.

IKK-α Has the Ability to Phosphorylate p73—To address whether IKK-α can phosphorylate p73, we performed an *in vitro* kinase assay. GST alone or the indicated GST-p73 deletion mutants (Fig. 11) were incubated with the active form of IKK-α in the presence of [γ-^{32}P]ATP. After incubation, the reaction mixture was separated by SDS-PAGE, followed by autoradiography. As shown in Fig. 11, GST-p73-(1–62) was phosphorylated by IKK-α, suggesting that the N-terminal region of p73 is phosphorylated by the active form of IKK-α.

DISCUSSION

Until recently, the IKK complex has been thought to participate in the cytoplasmic signaling pathway that activates NF-κB. However, this viewpoint has been challenged with the findings of the nuclear accumulation and function of IKK-α in response to cytokine exposure (33, 34). According to the previous results, nuclear IKK-α contributes to the induction of NF-κB-dependent gene expression through histone H3 phosphorylation. In this study, we found that CDDP treatment (DNA cross-linking) leads to a remarkable accumulation of IKK-α in the cell nucleus. We also demonstrated that IKK-α directly binds to the sequence-specific DNA-binding domain of p73α and has positive effects on its stability as well as pro-apoptotic function. The CDDP-induced stabilization of p73α was dependent on IKK-α as examined by siRNA-mediated knockdown and using IKK-$\alpha^{-/-}$ MEFs. In addition, chromatin immunoprecipitation assays showed that the IKK-α-dependent stabilization of p73α correlates with an increase in the amounts of p73α recruited onto the human *bax* promoter. Our present findings therefore imply not only a novel nuclear role of IKK-α in regulating the DNA damage response, which is distinct from NF-κB activation, but also a new regulatory pathway of pro-apoptotic p73α.

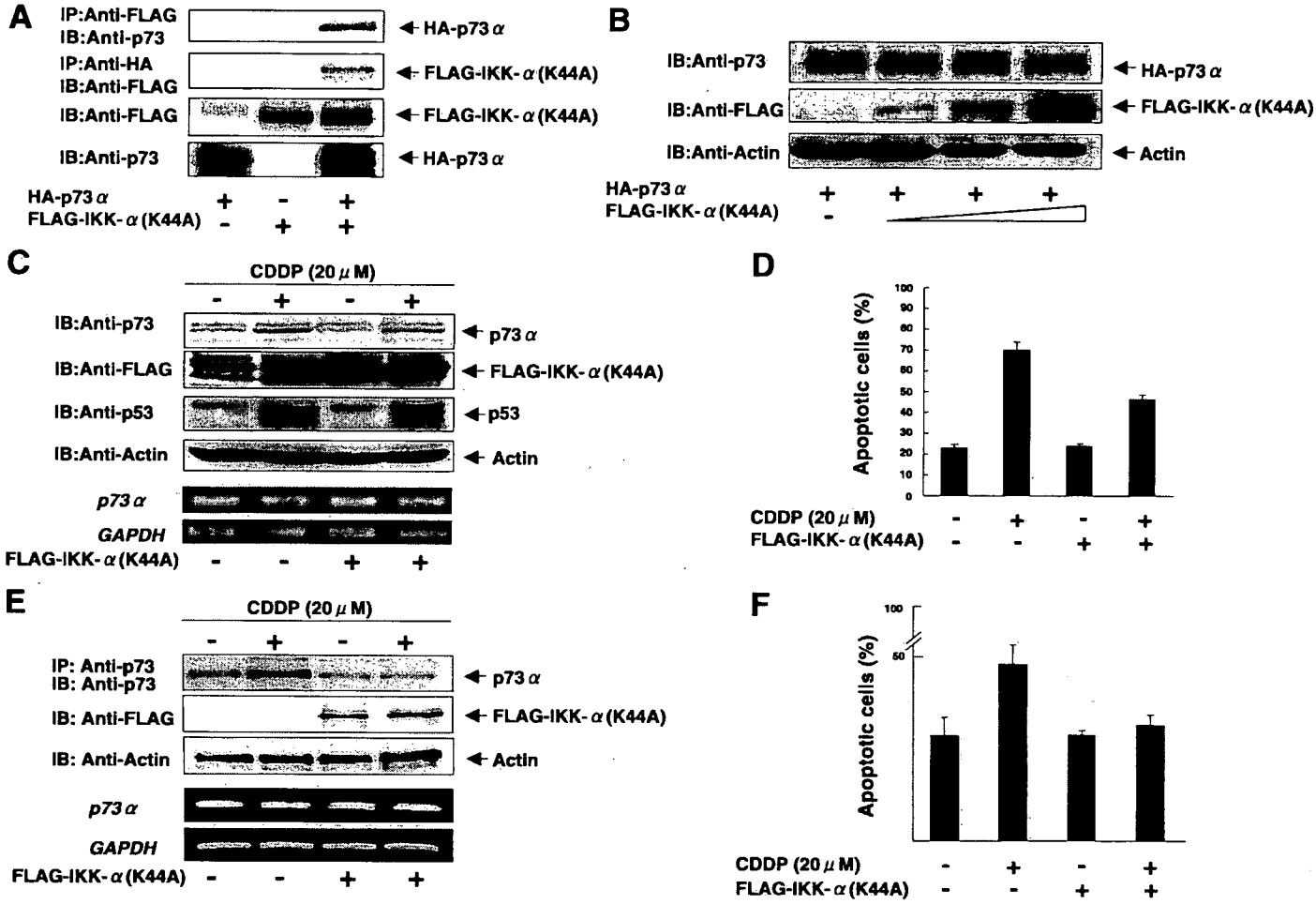

FIGURE 10. **Kinase-deficient IKK-α fails to stabilize p73α.** *A*, shown is the physical interaction between IKK-α(K44A) and p73α. COS-7 cells were transiently cotransfected with the indicated expression plasmids. Whole cell lysates were subjected to immunoprecipitation (*IP*) with anti-FLAG or anti-HA antibody, followed by immunoblotting (*IB*) with anti-p73 or anti-FLAG antibody, respectively. *B*, IKK-α(K44A) has no detectable effect on the amount of p73α. COS-7 cells were transiently cotransfected with the indicated combinations of expression plasmids. Equal amounts of the lysates were subjected to immunoblotting with anti-p73 or anti-FLAG antibody. *C*, IKK-α(K44A) suppresses endogenous p73 in response to CDDP. U2OS cells transiently transfected with or without FLAG-IKK-α(K44A) were left untreated or treated with CDDP for 24 h. Whole cell lysates and total RNA were prepared and subjected to immunoblotting (*upper panels*) or RT-PCR analysis (*lower panels*). *GAPDH*, glyceraldehyde-3-phosphate dehydrogenase. *D*, IKK-α(K44A) inhibits CDDP-induced apoptosis. U2OS cells transiently cotransfected with the β-galactosidase expression plasmid with or without the FLAG-IKK-α(K44A) expression plasmid were treated with CDDP for 24 h or left untreated. Cells were then subjected to double staining as described in the legend to Fig. 9. The percentage of transfected apoptotic cells is indicated. *E* and *F*, transfected H1299 cells were exposed to CDDP or left untreated and subjected to immunoprecipitation, followed by immunoblotting (*E*, *upper panels*), RT-PCR (*E*, *lower panels*), and apoptosis assays (*F*).

Previous studies have suggested that endogenous p73 is both stabilized and activated for apoptosis in response to CDDP and γ-ionizing irradiation through a pathway that depends on the nuclear non-receptor tyrosine kinase c-Abl (15–17). c-Abl binds to p73 via the P*XX*P motif of p73 and the c-Abl SH3 (Src homology 3) domain and phosphorylates p73 at Tyr^{99}. The phosphorylated form of p73 undergoes nuclear redistribution and becomes associated with the nuclear matrix in a c-Abl-dependent manner (36). In addition, HIPK2 (homeodomain-interacting protein kinase-2), which interacts with p73 and enhances its function, co-localizes with p73 in nuclear body-like structures (46). Mittnacht and Weinberg (47) reported that the retinoblastoma protein pRb differentially associates with the nuclear matrix, depending on its phosphorylation status or the integrity of the protein. The underphosphorylated form of pRb, which is active in growth control, remains tightly associated with the nuclear matrix, whereas the hyperphosphorylated form and a mutant form are detected largely in the nucleoplasm. In this study, we have demonstrated that IKK-α has the ability to stabilize and activate p73α and co-localizes with p73α in the nuclear lamina. Our findings, together with those previous observations, suggest that the nuclear structures including the nuclear matrix and/or nuclear body might provide an important subnuclear locale for p73 function.

As expected from their extensive amino acid sequence similarity, both IKK-α and IKK-β display IκB kinase activity *in vitro* (48), suggesting that their biochemical and biological functions seem to be redundant and overlapping with regard to NF-κB activation. On the other hand, genetic disruption studies in mice have demonstrated that IKK-α and IKK-β might have distinct regulatory functions. In IKK-α-deficient mice, inflammatory cytokine-induced activation of the NF-κB pathway is not severely impaired, although various developmental abnormalities, including defective epidermal differentiation, are detected (49–52). In contrast, mice lacking IKK-β die immedi-